SUPPORTING INFORMATION

G-Arylated Hydrogen-bonded Cyclic Tetramer Assemblies with Remarkable Thermodynamic and Kinetic Stability

Sonia Romero-Pérez,[†] Jorge Camacho-García,[†] Carlos Montoro-García,[†] Ana M. López-Pérez,[†] Alfredo Sanz,[†] María José Mayoral[†] and David González-Rodríguez*[,†]

[†] *Nanostructured Molecular Systems and Materials* Group, Departamento de Química Orgánica, Universidad Autónoma de Madrid, 28049 Madrid, Spain.

SUPPORTING INFORMATION

TABLE OF CONTENTS

1. Synthesis and Characterization S2
2. ^{1}H and ^{13}C NMR spectra of the compounds S8
3. Solvent-dependent ^{1}H NMR experiments. Figure S1 S18
4. EXSY spectra in DMF. Figure S2. S19
5. Concentration-dependent ^{1}H NMR experiments in polar solvents. Figure S3. S23
6. Temperature-dependent ^{1}H NMR experiments in polar solvents. Figure S4. S26
7. Concentration-dependent UV-vis and CD experiments in THF. Figure S5. S29
8. Temperature-dependent UV-vis and CD experiments in THF. Figure S6. S31
9. Overview of thermodynamic and kinetic parameters in different solvents. Table S3. S34

1. Synthesis and Characterization

General Methods

MALDI-TOF mass spectra were determined on a Ultraflex III (MALDI-TOF/TOF) of Bruker. Dithranol was employed as the solid matrix. **Electrospray mass spectra** were determined on a QSTAR of ABSciex. Methanol using 0.1% formic acid as ionising source. **NMR spectra** were recorded with a BRUKER AC-300 (300 MHz) instrument or BRUKER DRX-500 (500 MHz) instrument. The temperature was actively controlled at 298 K. Chemical shifts are measured in ppm using the signals of the deuterated solvent as the internal standard [$CHCl_3$, calibrated at 7.26 ppm (^1H) and 77.0 ppm (^{13}C); DMSO-d_6 calibrated at 2.50 ppm (^1H) and 39.5 ppm (^{13}C) and DMF-d_7 calibrated at 8.03 ppm (^1H)]. **Column chromatography** was carried out on silica gel Merck-60 (230-400 mesh, 60 Å), and TLC on aluminium sheets precoated with silica gel 60 F254 (Merck). **Circular Dichroism** and **Absorption** spectra were recorded with a JASCO V-815 equipment. The temperature was controlled using a JASCO Peltier thermostatted cell holder with a range of 263–383 K, adjustable temperature slope, and accuracy of ± 0.1 K. **Computational Details.** The structure of all compounds was build using the Hyperchem 8.0.3 software package (Hypercube, Inc.) for Windows and the geometry was pre-optimized using PM3 semiempirical calculations. They were then exported to the Gaussian 03 suite of programs (Gaussian 03W, Revision C.01, M. J. Frisch, et al.,Gaussian Inc., Wallingford CT, 2004) for further structural optimization by the density functional theory (DFT) approach, making use of Becke's three parameter B3LYP exchange-correlation functional and the 6-31G basis set.

Starting materials

Chemicals were purchased from commercial suppliers and used without further purification. Solid, hygroscopic reagents were dried in a vacuum oven before use. Reaction solvents were thoroughly dried before use using standard methods. The synthesis and characterization of compounds **G5**, **C1** and **GC_H** have been recently reported by us.[1] The synthesis of **GC_{Ar1}** and **GC_{Ar2}** are detailed below.

Synthetic procedures and characterization data

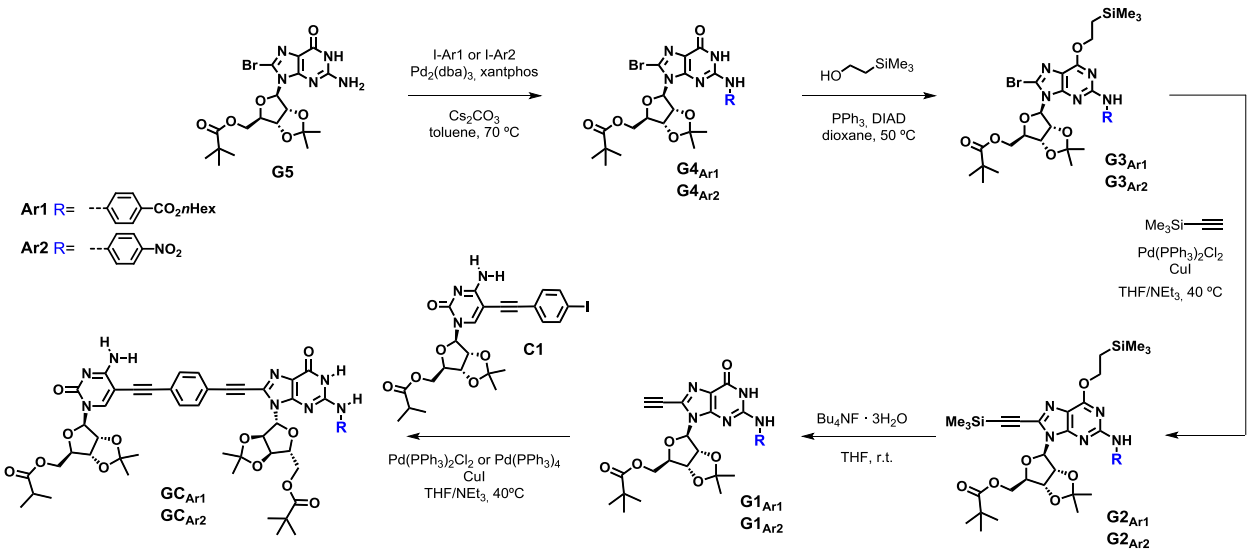

Scheme S1. Synthetic route to **GC_{Ar1}** and **GC_{Ar2}**.

[1] (a) Camacho-García, J.; Montoro-García, C.; López-Pérez, A. M.; Bilbao, N.; Romero-Pérez, S.; González-Rodríguez, D. *Org. Biomol. Chem.* **2015**, *13*, 4506–4513. (b) Montoro-García, C.; Camacho-García, J.; López-Pérez, A. M.; Bilbao, N.; Romero-Pérez, S.; Mayoral, M. J.; González-Rodríguez, D. *Ang. Chem. Int. Ed.* **2015**, DOI: 10.1002/anie.201501321.

Standard Procedures used in the Synthesis

***Standard Procedure A*. *N*-arylation Reaction.** The purine **G5**, $Pd_2(dba)_3$ (0.2 eq.), xantphos (0.2 eq.), Cs_2CO_3 (2 eq.) and the corresponding *p*-iodobenzene derivative (2 eq.) were suspended in dry toluene at 70°C under argon atmosphere. Once the reaction was complete, the mixture was filtrated over celite and solvents were removed under vacuum. The product was finally purified by column chromatography (eluent indicated in each case).

***Standard Procedure B*. Mitsunobu reaction to protect the carbonyl group.** The *N*-arylated nucleobase was dissolved in dioxane, together with PPh_3 (1.5 eq.) and was stirred at 50°C under argon atmosphere. Afterwards, DIAD (1.4 eq.) and trimethylsilylethanol (1.6 eq.) were added dropwise. The reaction was monitored by TLC until completion. Finally, solvents were removed under vacuum and the crude product was subjected to column chromatography (eluent indicated in each case).

***Standard Procedure C*. Sonogashira coupling with trimethylsilylacetilene.** The solvent mixture THF/NEt_3 (4:1) was subjected to deoxygenation by freeze-pump-thaw cycles. Then, this solvent was added over the reaction mixture containing the corresponding halogenated base (1 eq.), CuI (0.01 eq.) and $Pd(PPh_3)_2Cl_2$ (0.02 eq.). Subsequently, trimethylsilylacetylene (3 eq.) was added dropwise. The reaction was stirred at 40°C until completion, which was monitored by TLC. Thereafter, the mixture was filtrated over celite and solvents were evaporated at reduced pressure. The resulting crude product was purified by column chromatography (eluent indicated in each case).

***Standard procedure D*. Fluoride-sensitive groups deprotection.** Trihydrated tetrabutylammonium fluoride (1.5-2 eq.) was slowly added at room temperature to the corresponding nucleobase dissolved in THF. The mixture was stirred at room temperature until reaction completion. The solvent was evaporated at reduced pressure and the crude product was subjected to column chromatography (eluent indicated in each case).

***Standard Procedure E*. Sonogashira coupling between the ethynyl-purine and the iodinated pyrimidine.** A dry THF/NEt_3 (4:1) solvent mixture was subjected to deoxygenation by freeze-pump-thaw cycles. Afterwards, this solvent was added over the system containing the corresponding ethynyl-nucleobase (1.1 eq.), the iodinated pyrimidine **C1** (1 eq.), CuI (0.01 eq.) and $Pd(PPh_3)_2Cl_2$ (0.02 eq.) or $Pd(PPh_3)_3$ (0.02 eq.). The reaction was stirred under argon atmosphere at 50°C until completion, which was monitored by TLC. Subsequently, the mixture was filtrated over celite and the solvent was removed under vacuum. The resulting coupling product was isolated by column chromatography (eluent indicated in each case).

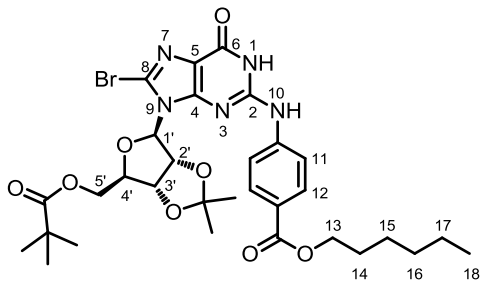

G4$_{Ar1}$. Following *Standard Procedure A*, the *N*-arylated product was synthesized from nucleobase **G5** (2.93 mmol, 1.42 g), hexyl-4-iodobenzoate (5.86 mmol, 1.95 g), $Pd_2(dba)_3$ (0.29 mmol, 268 mg), xantphos (8.79 x 10^{-2} mmol, 50 mg) and Cs_2CO_3 (5.86 mmol, 1.93 g) in 100 mL of dry toluene at 70°C. The crude product was purified by column chromatography ($CHCl_3$/MeOH 30:1), to yield 1.17 g of the purine (58%). **^{1}H NMR** (300 MHz, DMSO-d_6): δ (ppm) = 11.40 (s (b), 1H, NH^{1}), 9.50 (s (b), 1H, NH^{10}), 7.94 (d, J = 8.6 Hz, 2H, H^{12}), 7.63 (d, J = 8.6 Hz, 2H, H^{11}), 5.97 (d, J = 1.7 Hz, 1H, $H^{1'}$), 5.81 (d, J = 6.1 Hz, 1H, $H^{2'}$), 4.76 (dd, J = 3.7, 6.1 Hz, 1H, $H^{3'}$), 4.24 (t, J = 6.6 Hz, 2H, H^{13}), 4.18 (m, 1H, $H^{4'}$), 3.94 (dd, J = 11.6, 6.8 Hz, 1H, $H^{5'}$), 3.84 (dd, J = 11.7, 6.4 Hz, 1H, $H^{5'}$), 1.68 (q, J = 6.6 Hz, 2H, H^{14}), 1.53 (s, 3H, CH_3), 1.39 (s, 3H, CH_3), 1.30 (m, 6H, H^{15}, H^{16}, H^{17}), 0.94 (s, 9H, C(CH_3)$_3$), 0.86 (t, J = 6.6 Hz, 3H, H^{18}). **^{13}C NMR** (75 MHz, $CDCl_3$): δ (ppm) = 177.6, 166.1, 157.1, 151.2, 148.5, 142.1, 130.4, 125.4, 124.6, 119.4, 118.6, 114.2, 91.3, 84.6, 82.1, 81.7, 65.0, 62.4, 38.6, 31.7, 29.0, 27.1, 26.0, 25.4, 22.8, 14.2. **MS** (**MALDI-TOF):** *m/z* = 712.3 [M+Na]$^+$.

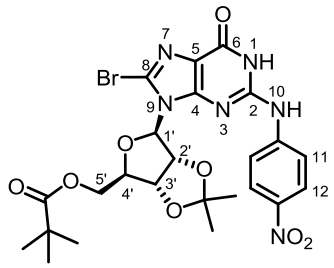

G4$_{Ar2}$. Following *Standard Procedure A*, the *N*-arylated product was obtained from guanosine **G5** (2.55 mmol, 1.24 g), *p*-iodonitrobenzene (5.11 mmol, 1.03 g), $Pd_2(dba)_3$ (0.51 mmol, 471 mg), xantphos (0.51 mmol, 298 mg) and Cs_2CO_3 (5.11 mmol, 1.69 g) in 95 mL of dry toluene at 70°C. The purification by column chromatography ($CHCl_3$/MeOH 40:1) afforded 481 mg (28%) of product. **^{1}H NMR** (300 MHz, $CDCl_3$): δ (ppm) = 11.51 (s (b), 1H, NH^{1}), 9.91 (s (b), 1H, NH^{10}), 8.13 (s (b), 4H, $H^{11, 12}$), 5.91 (m, 1H, $H^{1'}$), 5.40 (m, 1H, $H^{2'}$), 4.86 (m, 1H, $H^{3'}$), 4.29 (m, 1H, $H^{4'}$), 4.08 (s (b), 1H, $H^{5'}$), 3.99 (s (b), 1H, $H^{5'}$), 1.66 (s, 3H, CH_3), 1.53 (s, 3H, CH_3), 1.03 (s, 9H, C(CH_3)$_3$). **^{13}C NMR** (75 MHz, DMSO-D_6): δ (ppm) =176.8, 155.5, 153.7, 149.5, 124.8, 119.7, 114.0, 113.7, 113.2, 90.2, 83.5, 82.1, 80.9, 79.2, 64.0, 62.4, 38.0, 26.9, 26.8, 26.6, 26.0, 25.2. **MS** (**MALDI-TOF):** *m/z* = 629.2 [M+Na]$^+$.

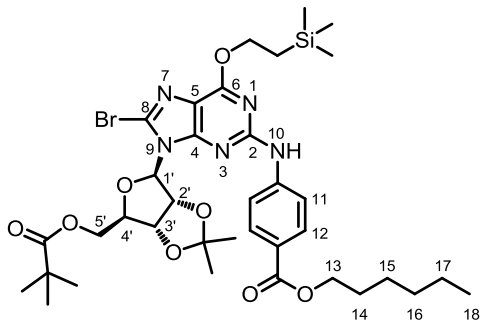

G3$_{Ar1}$. Following *Standard Procedure B*, the carbonyl protected nucleobase was synthesized from purine **G4$_{Ar1}$** (1.70 mmol, 1.17 g), PPh_3 (2.55 mmol, 668 mg), trimethylsilylethanol (2.72 mmol, 0.39 mL) and DIAD (2.38 mmol, 0.47 mL) in 15 mL of dry dioxane at 50°C under argon atmosphere. The resulting crude product was subjected to column chromatography (Hexane/AcOEt 4:1) to yield 1.50 g (99%) of **G3$_{Ar1}$**. **^{1}H NMR** (300 MHz, DMSO-d_6): δ (ppm) = 8.88 (s (b), 1H, NH^{10}), 7.91 (d, J = 8.8 Hz, 2H, H^{12}), 7.82 (d, J = 8.8 Hz, 2H, H^{11}), 6.05 (d, J = 1Hz, 1H, $H^{1'}$), 5.81 (d, J = 6.4 Hz, 1H, $H^{2'}$), 5.28 (dd, J = 6.2, 4.4 Hz, $H^{3'}$), 4.77 (m, 2H, CO-CH_2), 4.64 (m, 1H, $H^{4'}$), 4.25 (dd, J = 6.2, 4.4 Hz, 1H, $H^{5'}$), 4.23 (t, J = 6.5 Hz, 2H, H^{13}), 4.02 (dd, J = 6.2, 1.3 Hz, 1H, $H^{5'}$), 1.69 (m, 2H, H^{14}), 1.56 (s, 3H, CH_3), 1.41 (s, 3H, CH_3), 1.18 (m, 6H, H^{15}, H^{16}, H^{17}), 1.31 (t, J = 3.9 Hz, 2H, SiCH_2), 0.97 (s, 9H, C(CH_3)$_3$), 0.89 (t, J = 6.6 Hz, 3H, H^{18}), 0.10 (s, 9H, Si(CH_3)$_3$). **^{13}C NMR** (75 MHz, $CDCl_3$): δ (ppm) = 179.0, 166.5, 161.1, 155.6, 151.5, 144.3, 143.3, 133.6, 130.7, 129.0, 128.4, 123.4, 117.5, 116.6, 114.1, 90.6, 85.3, 84.2, 82.5, 65.9, 62.7, 39.0, 31.5, 28.7, 27.1, 25.7, 25.4, 22.6, 17.4, 14.0, -1.4.

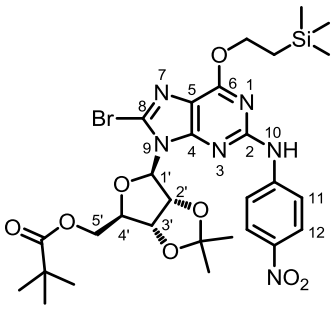

G3$_{Ar2}$. Following *Standard Procedure B*, the carbonyl protected product was synthesized from purine **G4$_{Ar2}$** (7.95 x 10^{-1} mmol, 0.48 g), PPh_3 (1.19 mmol, 0.31 g), trimethylsilylethanol (1.27 mmol, 0.18 mL) and DIAD (1.11 mmol, 0.22 mL) in 6 mL of dry dioxane at 50°C under argon atmosphere. The crude material was purified by column chromatography (Hexane/AcOEt 4:1), to yield 0.30 g (54%) of **G3$_{Ar2}$**. **^{1}H NMR** (300 MHz, $CDCl_3$): δ (ppm) = 8.71 (s, 1H, NH^{10}), 8.13 (d, J = 8.9 Hz, 2H, H^{12}), 7.83 (d, J = 8.9 Hz, 2H, H^{11}), 6.14 (d, J = 1.6 Hz, 1H, $H^{1'}$), 5.40 (dd, J = 1.6, 6.4 Hz, 1H, $H^{2'}$), 5.10 (m, 1H, $H^{3'}$), 4.88 (dd, J = 6.4, 3.1 Hz, $H^{4'}$), 4.63 (m, 2H, CO-CH_2), 4.45 (ddd, J = 9.3, 5.5, 3.1 Hz, 1H, $H^{5'}$), 3.81 (dd, J = 10.7, 5.5 Hz, 1H, $H^{5'}$), 1.56 (s, 3H, CH_3), 1.33 (s, 3H, CH_3), 1,25 (m, 2H, SiCH_2), 1.20 (s, 9H, C(CH_3)$_3$), 0.07 (s, 9H, Si(CH_3)$_3$). **^{13}C NMR** (75 MHz, DMSO-d_6): δ (ppm) = 179.7, 160.2, 154.4, 152.9, 146.4, 141.6, 126.8, 125.4, 117.6, 117.4, 114.5, 91.9, 86.2, 84.6, 82.7, 66.5, 62.6, 39.3, 31.1, 27.3, 27.2, 25.5, 22.2, 17.7, -1.2, -1.6. **MS** (**MALDI-TOF):** m/z = 729.2 [M+Na]$^+$.

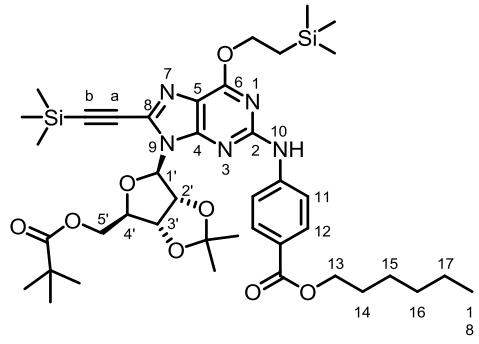

G2$_{Ar1}$ Following *Standard P*rocedure *C*, the purine was obtained from **G3$_{Ar1}$** (1.89 mmol, 1.50 g), $Pd(PPh_3)_2Cl_2$ (3.80 x 10^{-2} mmol, 26.60 mg), CuI (1.89 x 10^{-2}mmol, 3.6 mg) and trimethylsilylacetilne (5.67 mmol, 3.22 mL) in 15 mL of the THF/NEt_3 solvent at 40ºC. The mixture was stirred overnight. The crude material was subjected to column chromatography (Hexane/AcOEt 20:1) to yield 563 mg (44%) of the product. **^{1}H NMR** (300 MHz, $CDCl_3$): δ (ppm) = 8.14 (s (b), 1H, NH^{10}), 8.00 (d, J = 8.8 Hz, 2H, H^{12}), 7.76 (d, J = 8.8 Hz, 2H, H^{11}), 6.28 (d, J = 1.9 Hz, 1H, $H^{1'}$), 5.43 (dd, J = 1.9, 6.4 Hz, 1H, $H^{2'}$), 5.15 (d, J = 10.1 Hz, 1H, $H^{3'}$), 5.07 (dd, J = 6.4, 3.0 Hz, $H^{4'}$), 4.65 (m, 2H, CO-CH_2), 4.43 (ddd, J = 9.0, 5.8, 3.1 Hz, $H^{5'}$), 4.28 (t, J = 6.6 Hz, 2H, H^{13}), 3.88 (dd, J = 10.8, 5.8 Hz, 1H, $H^{5'}$), 1.74 (q, J = 6.7 Hz, 2H, H^{14}), 1.60 (s, 3H, CH_3), 1.37 (s, 3H, CH_3), 1.34 (m, 6H, H^{15}, H^{16}, H^{17}), 1.27 (m, 2H, SiCH_2), 1.21 (s, 9H, C(CH_3)$_3$), 0.91 (t, J = 6.6 Hz, 3H, H^{18}), 0.28 (s, 9H, Si(CH_3)$_3$), 0.012 (s, 9H, Si(CH_3)$_3$). **^{13}C NMR** (75 MHz, $CDCl_3$): δ (ppm) = 179.1, 166.6, 161.3, 155.8, 151.6, 144.4, 143.5, 133.8, 130.8, 125.5, 123.6, 117.6, 116.7, 114.2, 103.4, 92.6, 90.7, 85.4, 84.4, 82.7, 66.1, 62.9, 39.1, 31.7, 27.3, 25.6, 22.7, 17.6, 14.2, -0.4, -1.2. **MS** (**MALDI-TOF):** m/z = 830.5 [M+Na]$^+$.

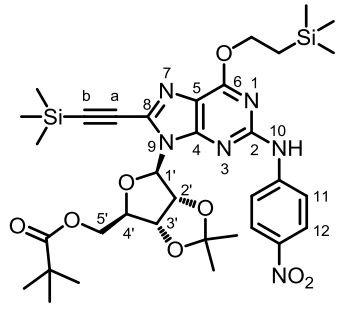

G2$_{Ar2}$. Following *Standard P*rocedure *C*, the product was synthesized from **G3$_{Ar2}$** (0.42 mmol, 295 mg), $Pd(PPh_3)_2Cl_2$ (8.32 x 10^{-3} mmol, 5.85 mg), CuI (4.16 x 10^{-3} mmol, 0.79 mg) and trimethylsilylacetilene (1.25 mmol, 0.18 mL) in 3 mL of the mixture THF/NEt_3 at 40ºC. The reaction was stirred for 24 hours. The crude product was purified by column chromatography (Hexane/AcOEt 8:1), to afford 192 mg (65%) of **G2$_{Ar2}$**. **^{1}H NMR** (300 MHz, $CDCl_3$): δ (ppm) = 8.66 (s, 1H, NH^{10}), 8.21 (d, J = 9.2 Hz, 2H, H^{12}), 7.90 (d, J = 9.2 Hz, 2H, 2H^{11}), 6.32 (d, J = 1.8 Hz, 1H, $H^{1'}$), 5.34 (m, 2H, $H^{2'}$, $H^{3'}$), 5.08 (dd, J = 3.0, 6.4 Hz, 1H, $H^{4'}$), 4.70 (m, 2H, CO-CH_2), 4.47 (ddd, J = 9.3, 5.7, 3.0 Hz, 1H, $H^{5'}$), 3.87 (dd, J = 10.7, 5.7 Hz, 1H, $H^{5'}$), 1.62 (s, 3H, CH_3), 1.38 (s, 3H, CH_3), 1.30 (m, 2H, SiCH_2), 1.27 (s, 9H, C(CH_3)$_3$), 0.30 (s, 9H, Si(CH_3)$_3$), 0.13 (s, 9H, Si(CH_3)$_3$). **^{13}C NMR** (75 MHz, $CDCl_3$): δ (ppm) = 179.7, 161.5, 155.4, 151.6, 146.4, 141.6, 133.3, 125.4, 117.5, 117.4, 114.4, 101.1, 90.7, 86.1, 84.4,

82.7, 72.4, 66.5, 62.7, 39.3, 31.1, 27.3, 25.5, 22.1, 17.6, -0.4, -1.2, -1.6. **MS** (**MALDI-TOF):** *m/z* = 747.4 $[M+Na]^+$.

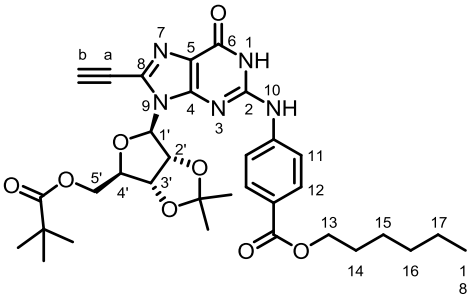

$G1_{Ar1}$. Following *Standard P*rocedure *D*, the deprotected guanosine was synthesized from **$G2_{Ar1}$** (0.43 mmol, 350 mg) and TBAF·$3H_2O$ (0.65 mmol, 205 mg) in 10 mL of THF. The crude product was purified by column chromatography ($CHCl_3$/MeOH 30:1) to yield 145 mg (53%) of **$G1_{Ar1}$**. **^{1}H RMN** (300 MHz, DMSO-d_6): δ (ppm) = 11.67 (s (b), 1H, NH^1), 9.93 (s (b), 1H, NH^{10}), 7.95 (d, J = 8.8 Hz, 2H, H^{12}), 7.69 (d, J = 8.8 Hz, 2H, H^{11}), 6.09 (d, J = 1.6 Hz, 1H, H$^{1'}$), 5.78 (d, J = 6.4 Hz, H$^{2'}$), 4.90 (s, 1H, H^b), 4.83 (dt, J = 5.9, 3.5 Hz, 1H, $H^{3'}$), 4.24 (t, J = 6.2 Hz, 2H, H^{13}), 4.18 (t, J = 5.0 Hz, $H^{4'}$), 3.92 (m, 2H, $H^{5'}$), 1.69 (q, J = 6.7 Hz, 2H, H^{14}), 1.54 (s, 3H, CH_3), 1.40 (s, 3H, CH_3), 1.32 (m, 6H, H^{15}, H^{16}, H^{17}), 0.94 (s, 9H, C(CH_3)$_3$), 0.89 (t, J = 6.4 Hz, 3H, H^{18}). **^{13}C NMR** (75 MHz, $CDCl_3$): δ (ppm) = 177.9, 166.2, 158.1, 150.0, 149.7, 142.2, 130.4, 119.0, 114.5, 90.2, 84.4, 82.9, 81.9, 66.0, 65.0, 38.7, 31.7, 31.1, 28.9, 27.2, 27.0, 25.9, 25.4, 22.8, 15.4. **HRMS (ESI+)**: Calculated for $C_{33}H_{42}N_5O_8$: 636.2955 $[M+H]^+$. Found: 636.3047 $[M+H]^+$.

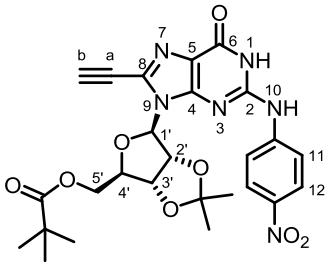

$G1_{Ar2}$. Following *Standard P*rocedure *D*, the deprotected purine was synthesized from **$G2_{Ar1}$** (0.27 mmol, 192 mg) and TBAF·$3H_2O$ (0.34 mmol, 109 mg) in 7 mL of THF. The crude material was subjected to column chromatography ($CHCl_3$/MeOH 15:1) to yield 134 mg (92%) of **$G1_{Ar2}$**. **^{1}H NMR** (300 MHz, DMSO-d_6): δ (ppm) = 11.52 (s (b), 1H, NH^1), 10.24 (s (b), 1H, NH^{10}), 8.22 (d, J = 8.7 Hz, H^{12}), 7.80 (d, J = 8.7 Hz, H^{11}), 6.10 (d, J = 2.1 Hz, 1H, $H^{1'}$), 5.73 (dd, J = 7.3, 2.2 Hz, $H^{2'}$), 4.92 (s, 1H, H^b), 4.86 (m, 1H, $H^{3'}$), 4.24 (d, J = 8.1 Hz, 1H, $H^{4'}$), 3.99 (m, 2H, $H^{5'}$), 1.56 (s, 3H, CH_3), 1.41 (s, 3H, CH_3), 0.96 (s, 9H, C(CH_3)$_3$). **^{13}C NMR** (126 MHz, DMSO-D_6): δ (ppm) = 176.8, 166.9, 131.7, 131.4, 128.6, 124.7, 119.5, 113.8, 89.1, 86.7, 83.2, 82.3, 81.0, 79.1, 72.7, 69.8, 62.6, 61.3, 38.0, 30.6, 29.0, 26.9, 26.5, 25.2, 21.8, 13.8. **HRMS (ESI+)**: Calculated for $C_{26}H_{29}N_6O_8$: 553.1969 $[M+H]^+$. Found: 553.2057 $[M+H]^+$.

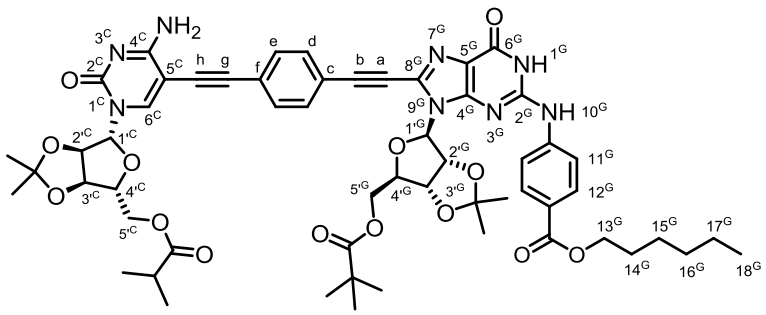

GC_{Ar1}. Following the *Standard P*rocedure *E*, the final compound was synthesized from **$G1_{Ar1}$** (0.19 mmol, 111 mg), $Pd(PPh_3)_4$ (3.80 x 10^{-3}mmol, 4.40 mg), CuI (1.90 x 10^{-3}mmol, 0.36 mg) and the cytidine **C1** equipped with the spacer (0.23 mmol, 145 mg) in 5 mL of the solvent THF/NEt_3. The mixture was stirred at 40ºC overnight. The coupling product was isolated by column chromatography ($CHCl_3$/MeOH 30:1) to yield 137 mg (66%) of **GC_{Ar1}**. **^{1}H NMR** (300 MHz, DMSO-d_6): δ (ppm) = 11.27 (s (b), 1H, NH^{1G}), 9.43 (s (b), 1H, NH^{10G}), 8.14 (s, 1H, H^{6C}), 7.99 (s, 1H, NH^{4C}), 7.95 (d, J = 8.5 Hz, 2H, H^{12G}), 7.69 (s (b), 4H, $H^{d,e}$), 7.65 (d, J = 8.5 Hz, 2H, H^{12G}), 7.30 (s, 1H, NH^{4C}), 6.18 (d, J = 1.9 Hz, 1H,

$H^{1'G}$), 5.82 (s, 1H, $H^{1'C}$), 5.78 (d, J = 6.3 Hz, 1H, $H^{2'G}$), 5.02 (dd, J = 1.9, 6.5 Hz, 1H, $H^{2'C}$), 4.82 (m, 2H, H^{13}), 4.25 (m, 6H, $H^{3'G}$, $H^{3'C}$, $H^{4'G}$, $H^{4'C}$, $H^{5'G}$), 3.92 (m, 2H, $H^{5'C}$), 2.57 (q, J = 6.9 Hz, 1H, COCH(CH_3)$_2$), 1.68 (q, J = 6.8 Hz, 2H, H^{14G}), 1.55 (s, 3H, CH_3), 1.49 (s, 3H, CH_3), 1.40 (s, 3H, CH_3), 1.30 (m, 9H, CH_3, H^{15G}, H^{16G}, H^{17G}), 1.08 (dd, J = 7.0, 2.2 Hz, 6H, COCH(CH_3)$_2$), 0.89 (s, 9H, C(CH_3)$_3$), 0.85 (t, J = 6.8 Hz, 3H, H^{18G}). **^{13}C NMR** (75 MHz, $CDCl_3$): δ (ppm) = 178.5, 176.3, 166.3, 165.0, 159.2, 155.9, 150.1, 149.1, 145.8, 143.2, 132.1, 131.9, 131.7, 130.5, 125.6, 121.7, 121.3, 121.0, 120.5, 114.2, 114.0, 96.5, 96.0, 94.7, 93.2, 90.5, 86.0, 85.6, 83.9, 82.8, 82.1, 80.3, 80.2, 77.4, 65.1, 65.0, 64.0, 38.8, 33.8, 31.7, 29.0, 27.6, 27.3, 27.0, 26.2, 26.0, 25.0, 22.8, 19.1, 18.9, 14.2. **HRMS (MALDI-TOF)**: Calculated for $NaC_{57}H_{66}N_8O_{14}$: 1109.4591 $[M+Na]^+$. Found: 1109.4564 $[M+Na]^+$.

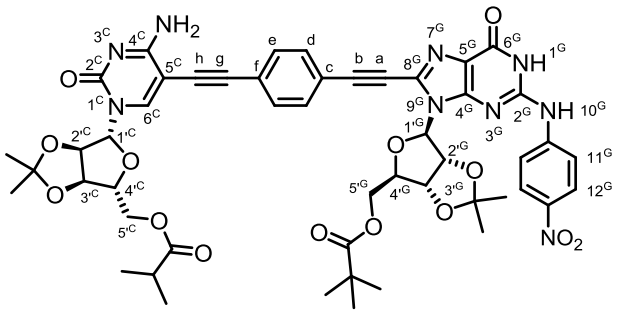

GC$_{Ar2}$. Following the *Standard P*rocedure *E*, the final compound was synthesized from **G1$_{Ar2}$** (0.24 mmol, 133 mg), $Pd(PPh_3)_2Cl_2$ (4.82×10^{-3} mmol, 3.38 mg), CuI (4.82×10^{-3} mmol, 0.46 mg) and the cytidine **C1** equipped with the spacer (0.27 mmol, 154 mg) in 6 mL of the solvent THF/NEt_3. The reaction was stirred at 40ºC for 18 hours. The coupling product was isolated by column chromatography ($CHCl_3$/AcOEt/MeOH 12:8:1) to yield 125 mg (51%) of **GC$_{Ar2}$**. **^{1}H NMR** (300 MHz, DMSO-d_6): δ (ppm) = 12.14 (s (b), 1H, NH^{1G}), 11.01 (s (b), 1H, NH^{10G}), 8.20 (d, J = 8.9 Hz, 2H, H^{12G}), 8.15 (s, 1H, H^{6C}), 8.00 (s (b), 1H, NH^{4C}), 7.83 (d, J = 8.8 Hz, 2H, H^{11G}), 7.70 (s (b), 4H, $H^{d,e}$), 7.31 (s (b), 1H, NH^{4C}), 6.20 (d, J = 2.1 Hz, 1H, $H^{1'G}$), 5.81 (m, 2H, $H^{1'C}$, $H^{2'G}$), 5.02 (dd, J = 6.4, 1.8 Hz, 1H, $H^{2'C}$), 4.92 (t, J = 4.9 Hz, 1H, $H^{3'G}$), 4.83 (dd, J = 6.7, 3.0 Hz, 1H, $H^{3'C}$), 4.26 (m, 4H, $H^{4'G}$, $H^{4'C}$, $H^{5'G}$), 3.99 (m, 2H, $H^{5'C}$), 2.59 (m, 1H, COCH(CH_3)$_2$), 1.58 (s, 3H, CH_3), 1.49 (s, 3H, CH_3), 1.45 (s, 3H, CH_3), 1.30 (s, 3H, CH_3), 1.08 (dd, J = 7.0, 2.2 Hz, 6H, COCH(CH_3)$_2$), 0.94 (s, 9H, C(CH_3)$_3$). **^{13}C NMR** (126 MHz, $CDCl_3$): δ (ppm) = 178.4, 176.2, 164.9, 159.1, 156.0, 149.4, 148.9, 145.4, 142.9, 132.2, 131.9, 131.6, 124.8, 121.8, 121.3, 121.0, 119.9, 114.8, 114.1, 96.1, 95.8, 94.8, 93.1, 90.2, 86.0, 85.6, 84.7, 83.4, 82.5, 81.7, 80.4, 80.3, 64.4, 63.8, 38.9, 33.9, 31.0, 29.8, 27.7, 27.2, 26.0, 25.3, 19.1, 18.9, 14.2. **HRMS (MALDI-TOF)**: Calculated for $NaC_{50}H_{53}N_9O_{14}$: 1026.3604 $[M+Na]^+$. Found: 1026.3593 $[M+Na]^+$.

2. ^{1}H and ^{13}C NMR spectra of the compounds

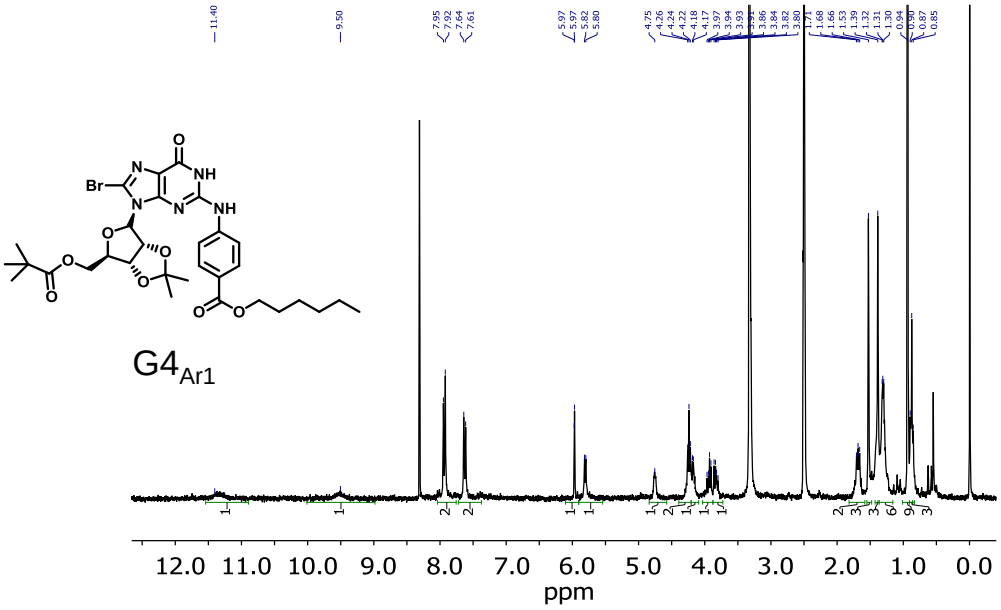

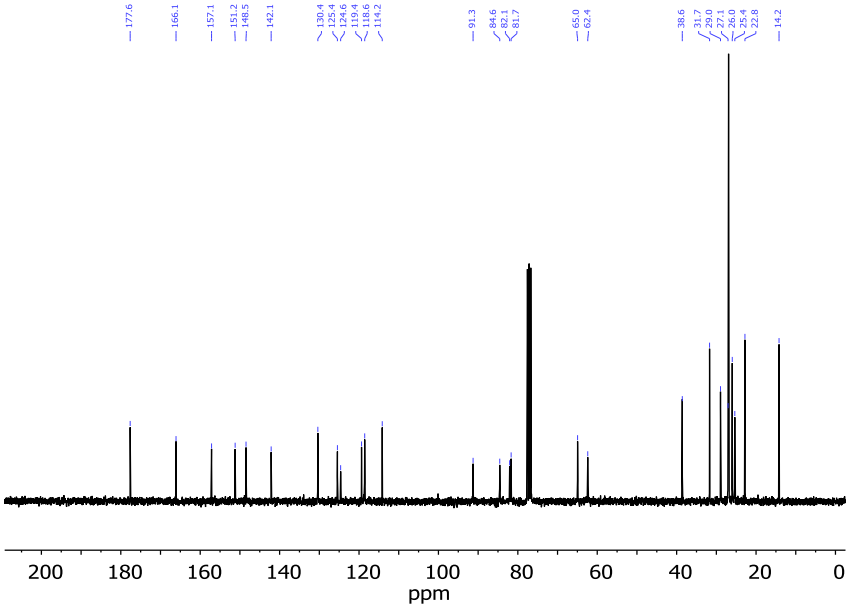

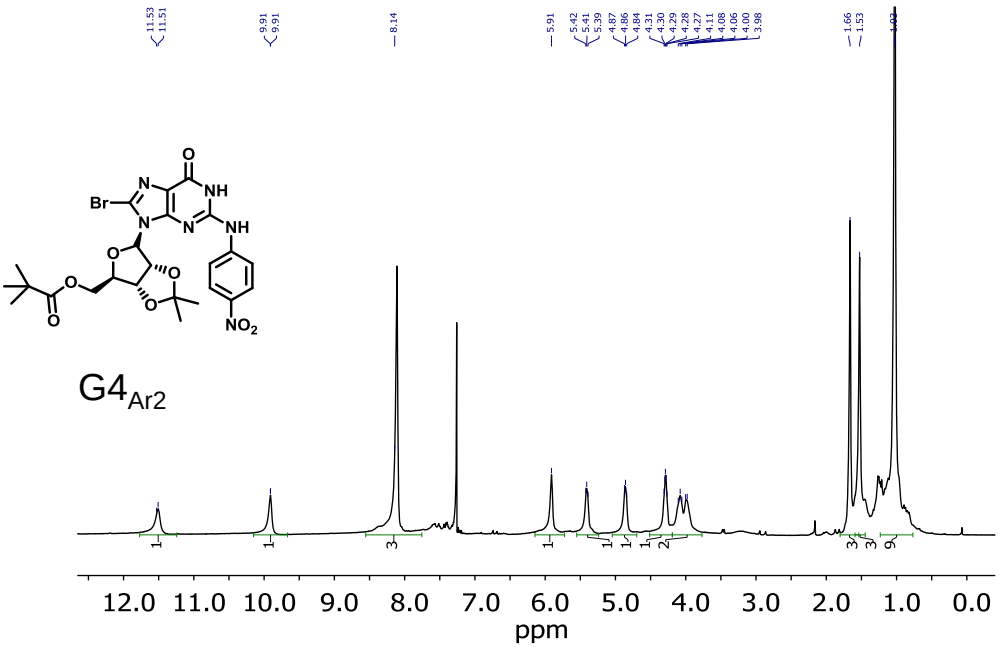
G4Ar2
ppm

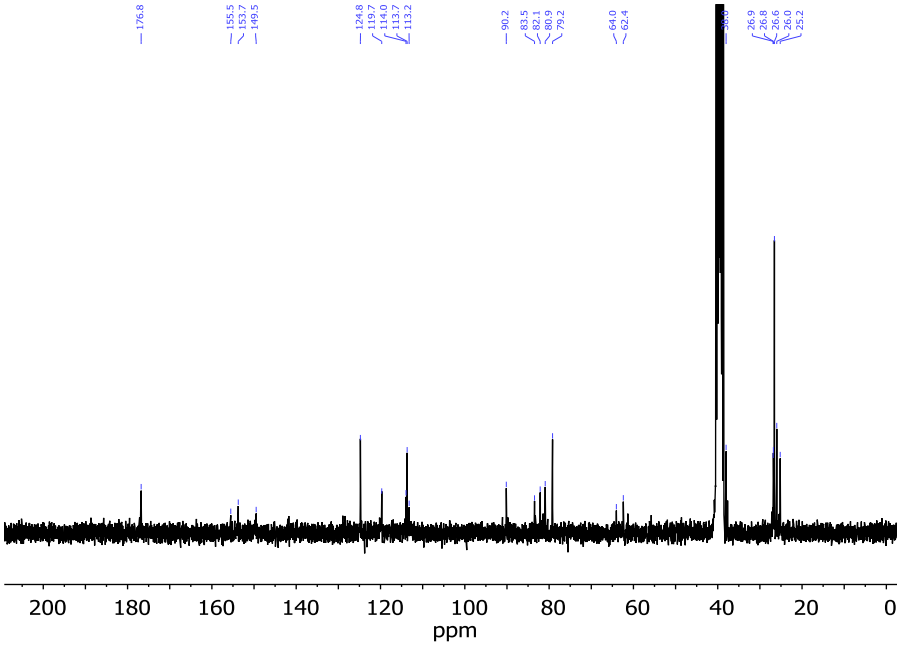
ppm

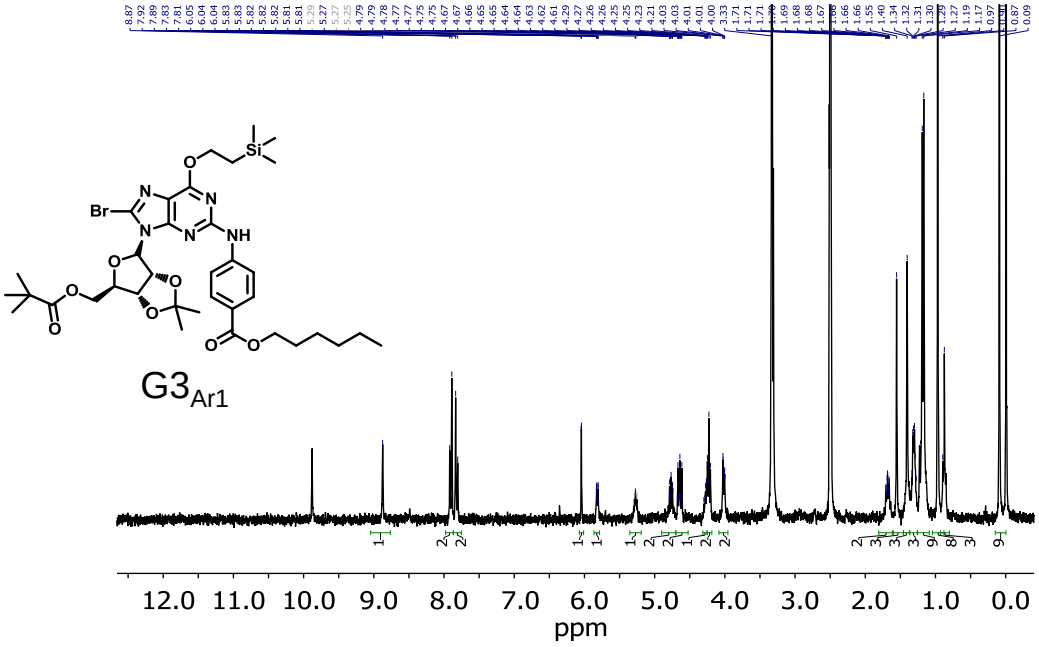
G3Ar1
12.0 11.0 10.0 9.0 8.0 7.0 6.0 5.0 4.0 3.0 2.0 1.0 0.0
ppm

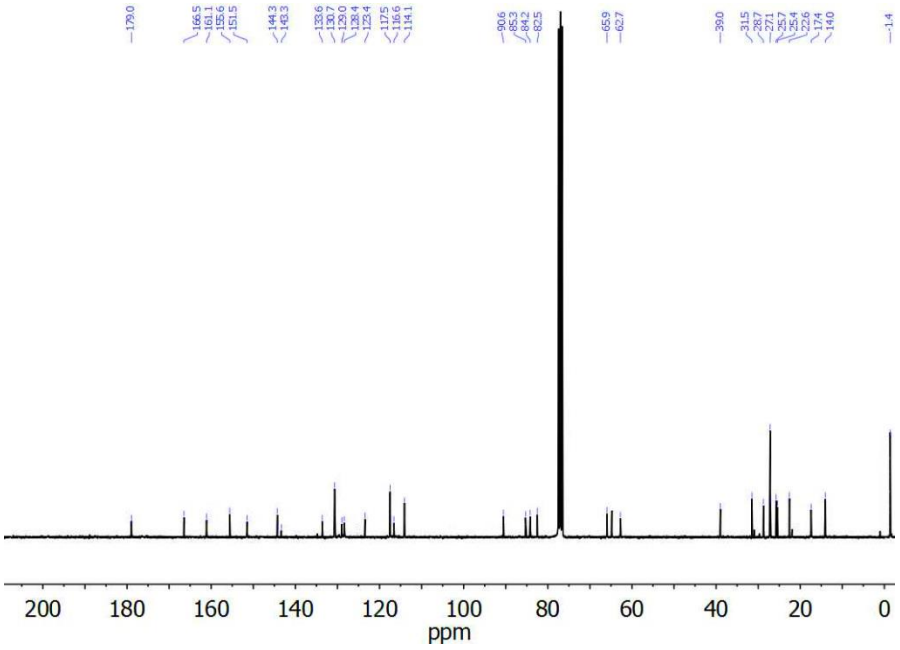
200 180 160 140 120 100 80 60 40 20 0
ppm

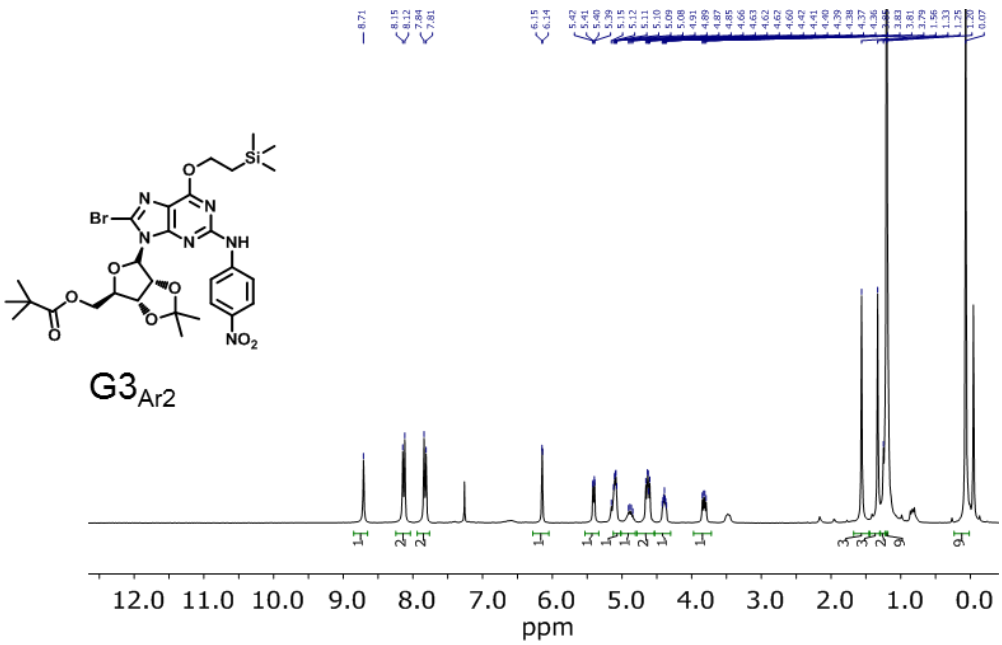
Br
N
N
N
N
O
Si
NH
O
O
O
O
O
NO2
G3Ar2
ppm

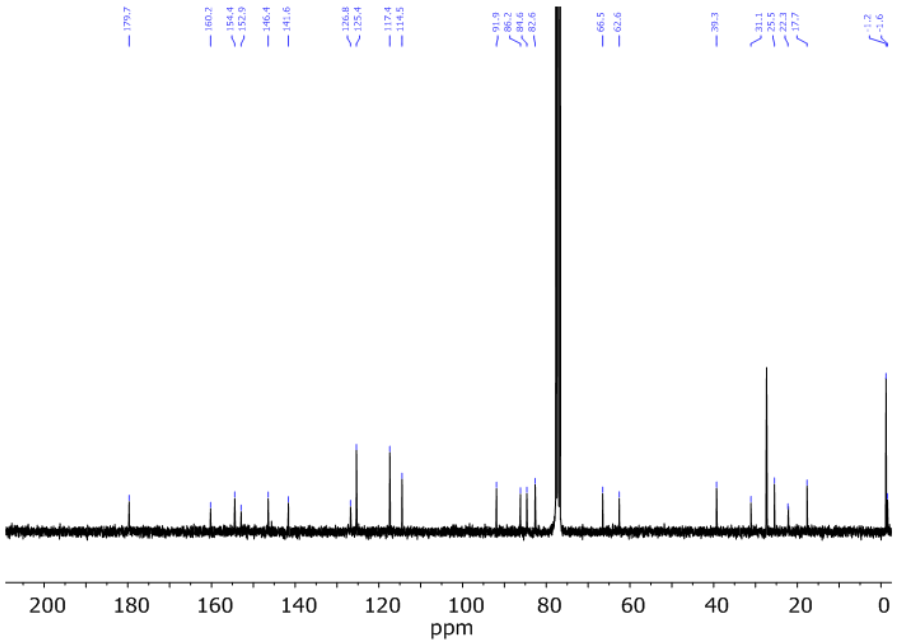
ppm

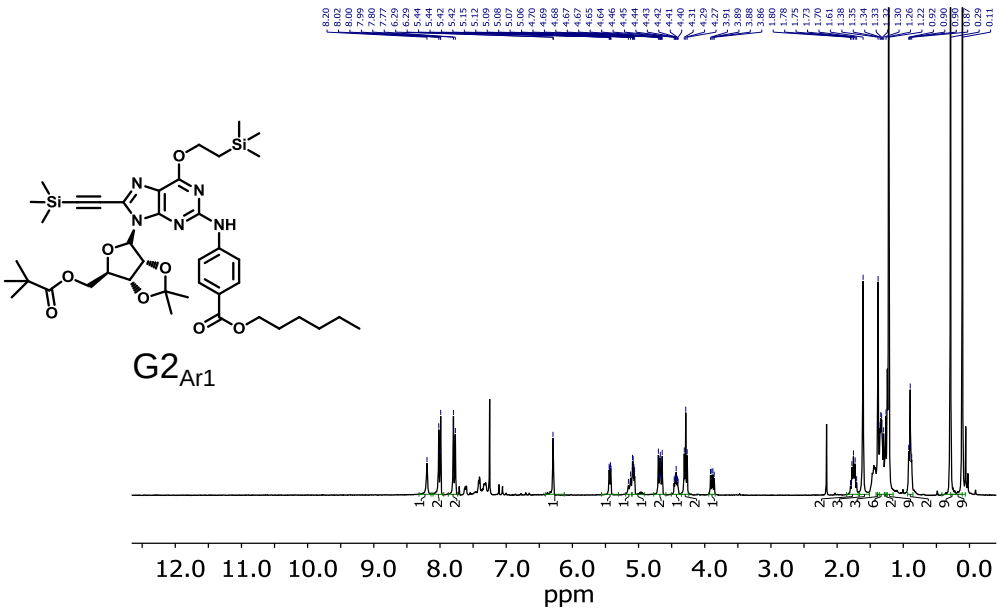
G2Ar1
12.0 11.0 10.0 9.0 8.0 7.0 6.0 5.0 4.0 3.0 2.0 1.0 0.0
ppm

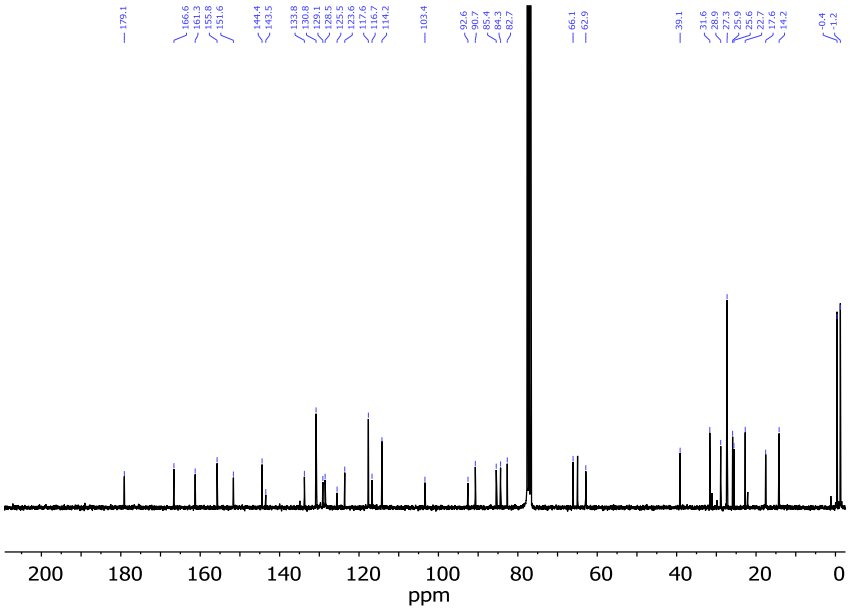
200 180 160 140 120 100 80 60 40 20 0
ppm

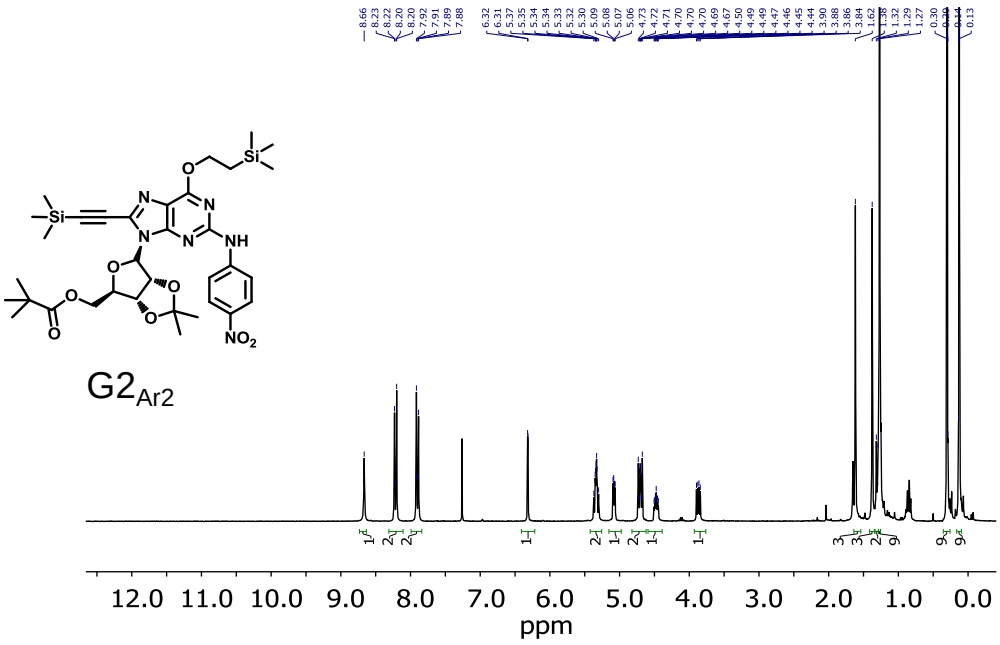
G2Ar2
12.0 11.0 10.0 9.0 8.0 7.0 6.0 5.0 4.0 3.0 2.0 1.0 0.0
ppm

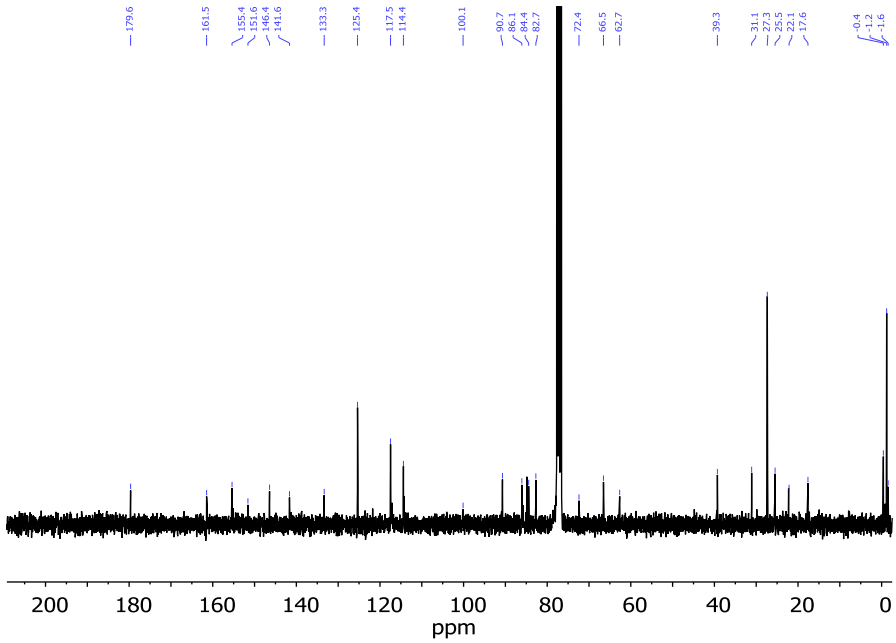
200 180 160 140 120 100 80 60 40 20 0
ppm

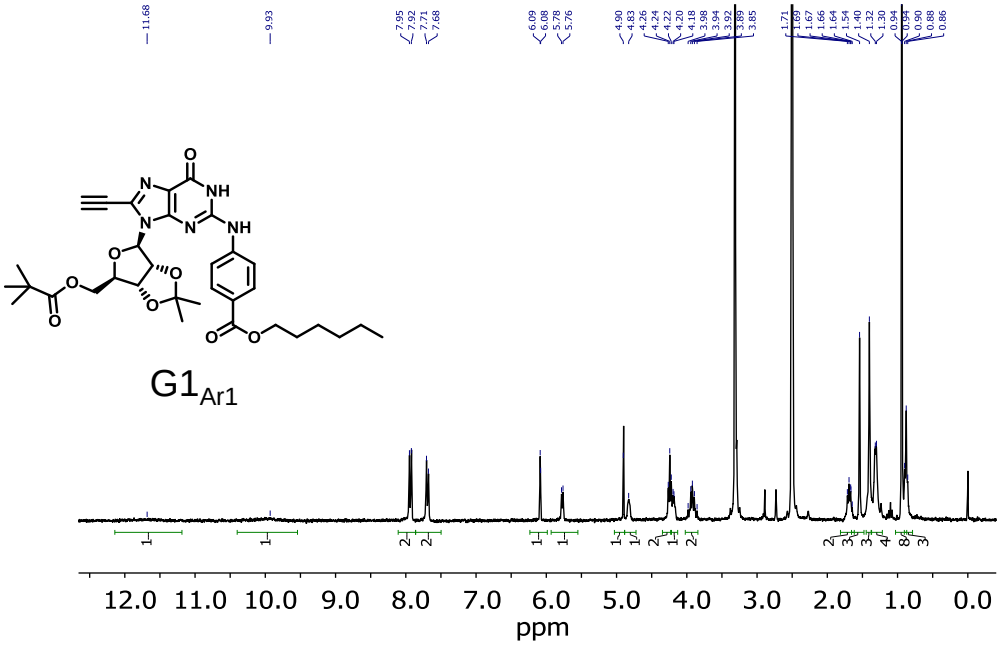
G1Ar1
ppm

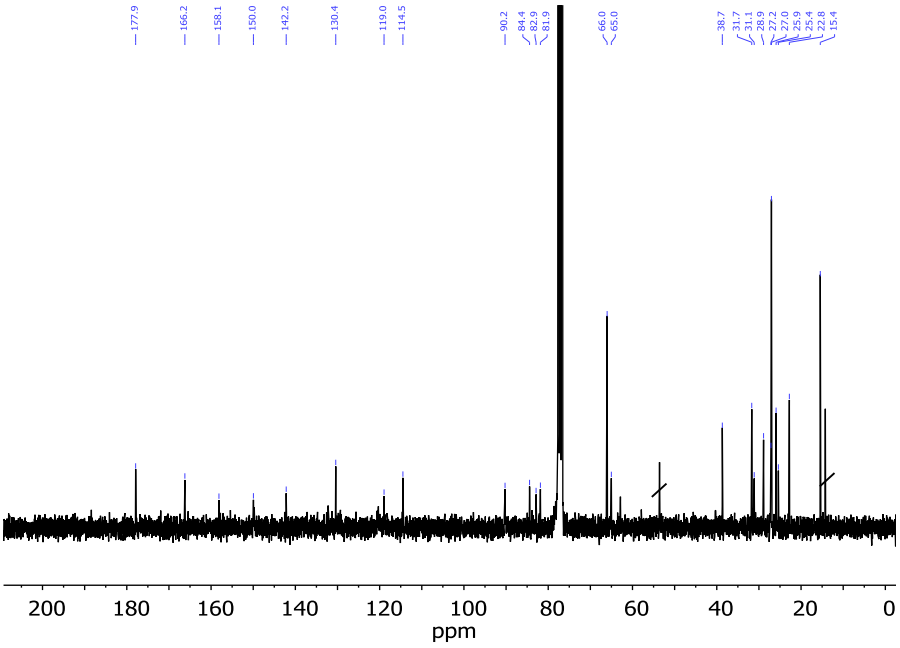
ppm

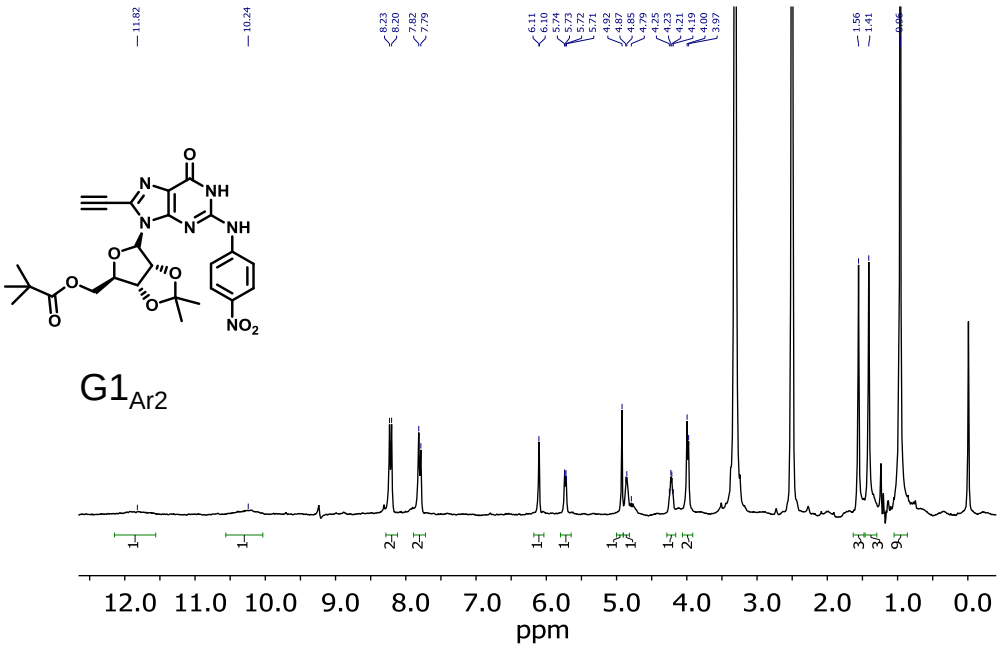
G1Ar2
ppm

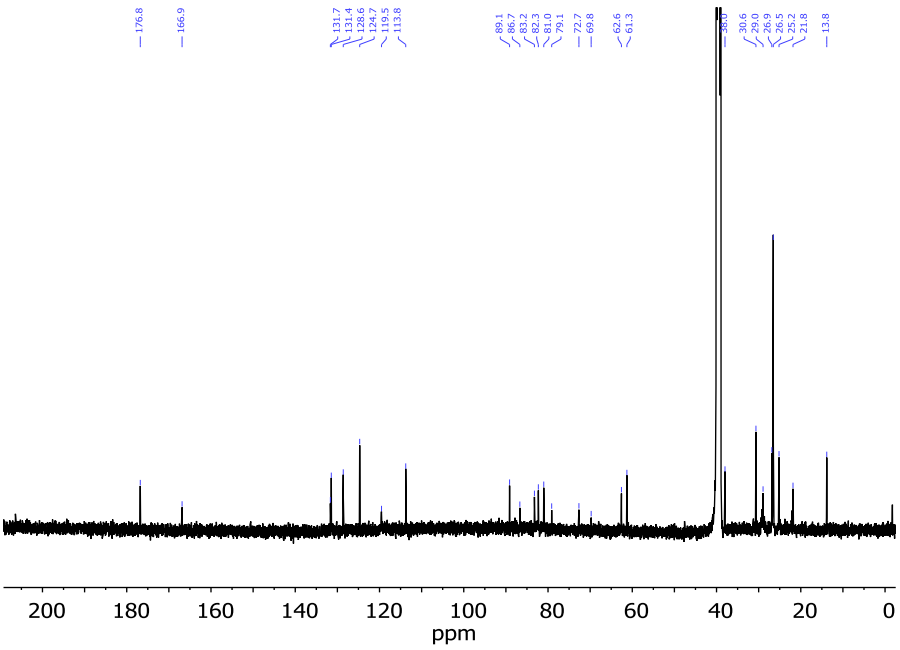
ppm

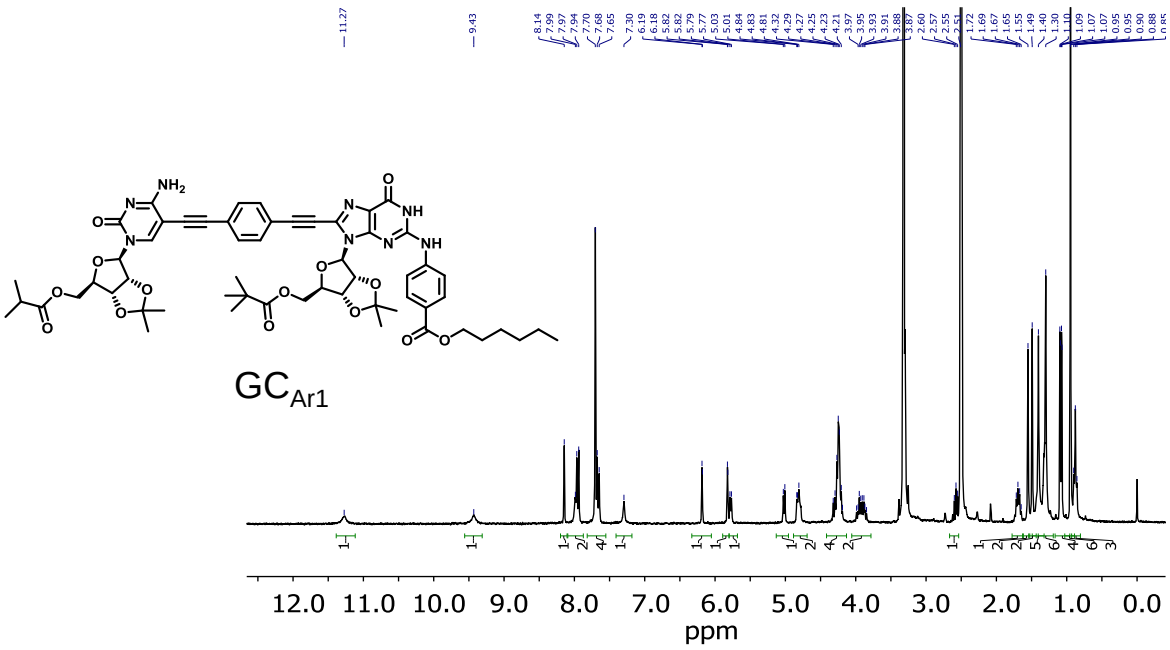
GCAr1
12.0 11.0 10.0 9.0 8.0 7.0 6.0 5.0 4.0 3.0 2.0 1.0 0.0
ppm

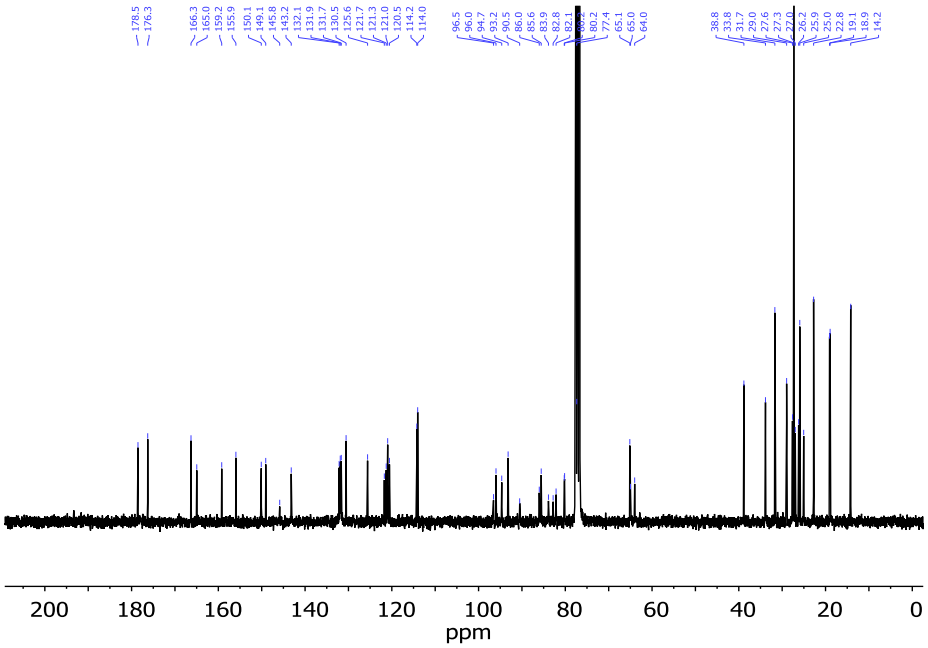
200 180 160 140 120 100 80 60 40 20 0
ppm

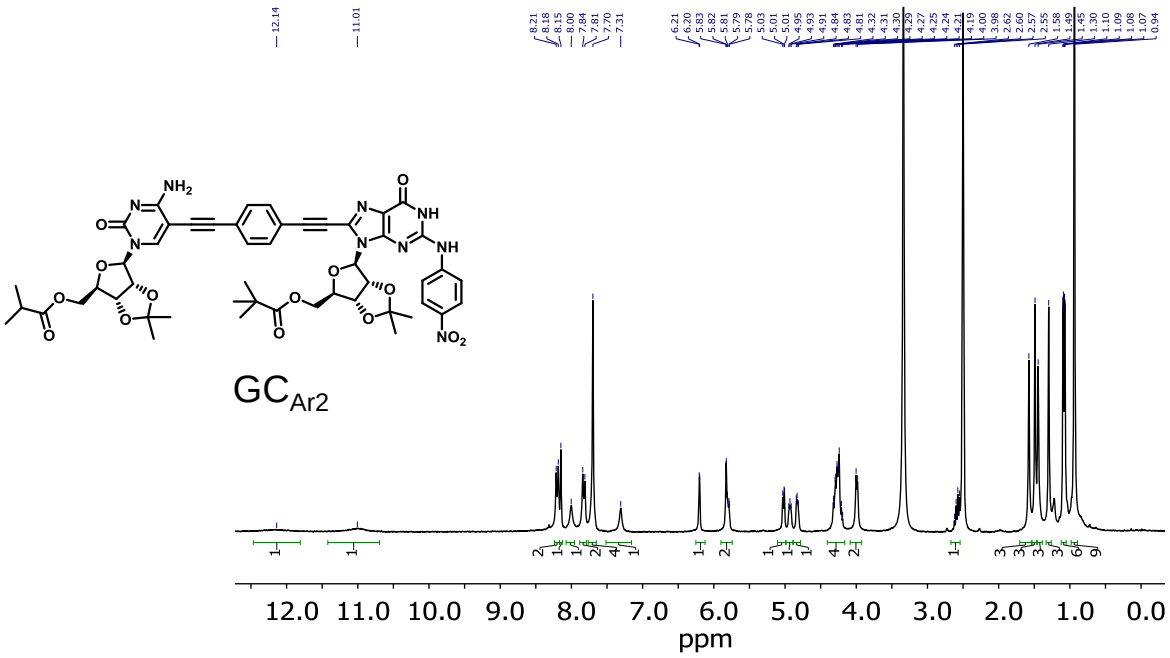
GC$_{Ar2}$
ppm

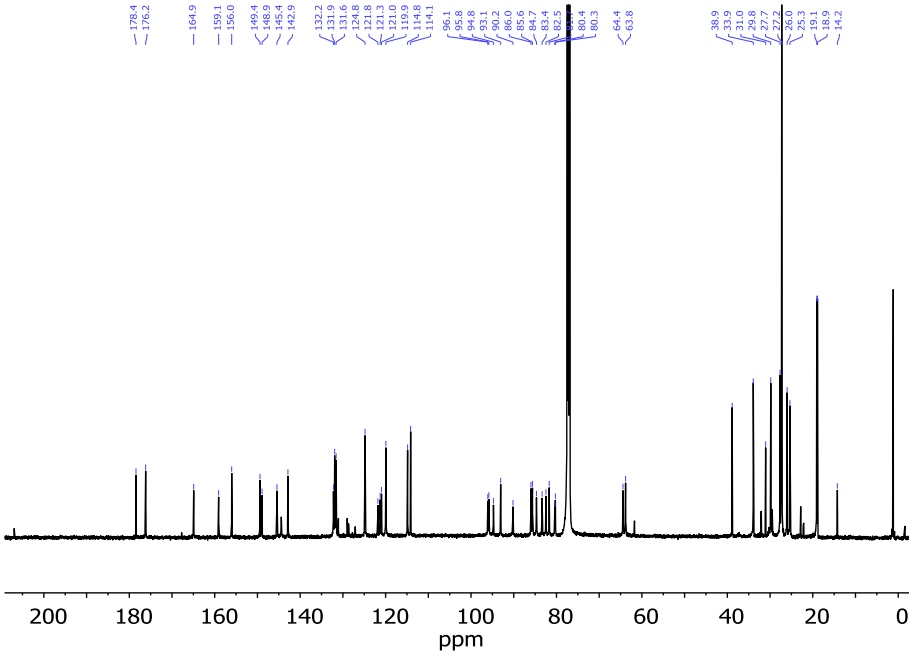
ppm

3. Solvent-dependent ^{1}H NMR experiments. Figure S1.

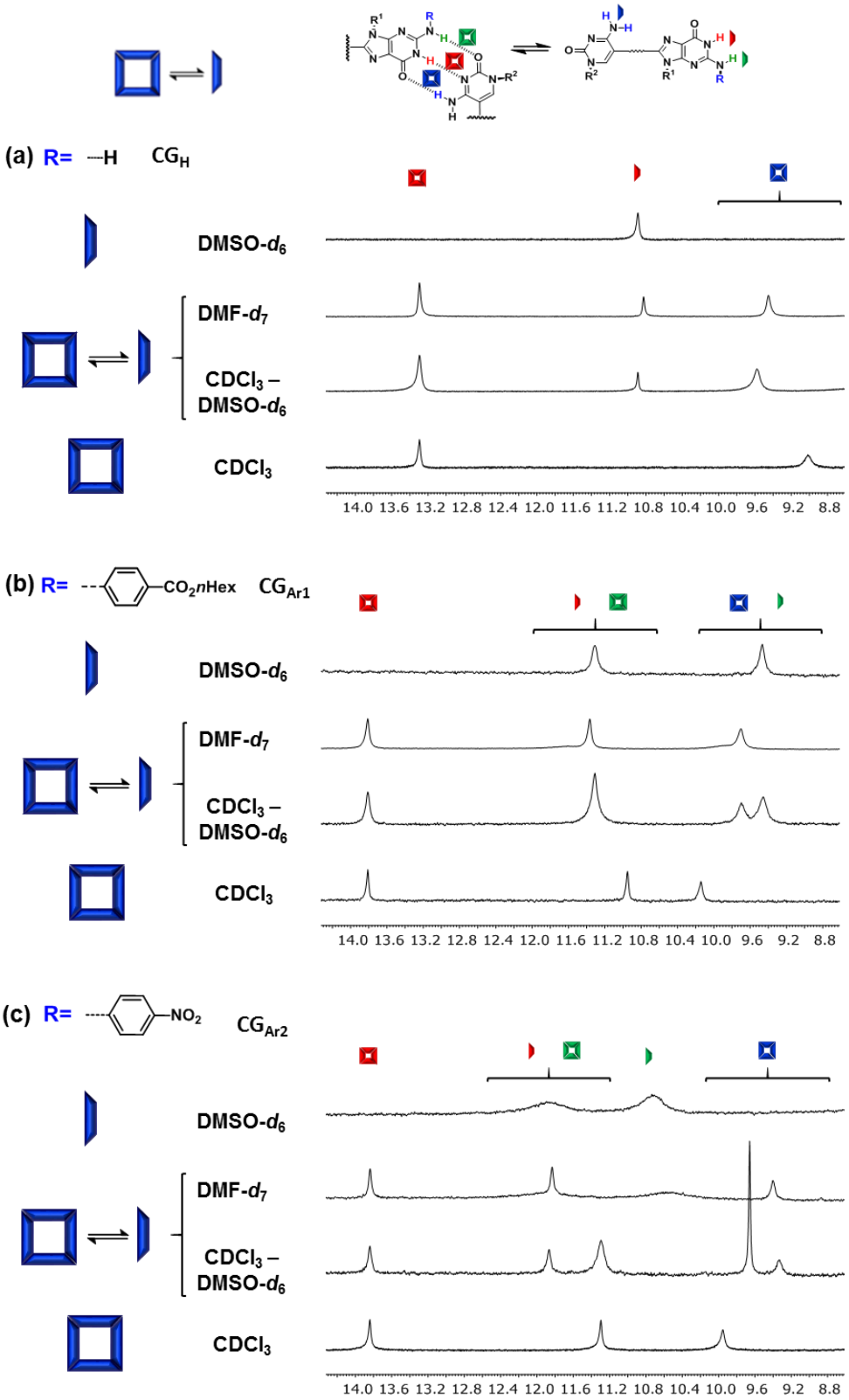

Figure S1. Downfield region of the ^{1}H NMR spectra of (**a**) **GC$_H$**, (**b**) **GC$_{Ar1}$** and (**c**) **GC$_{Ar2}$** in different solvents (*C* = *ca.* 10^{-2} M, *T* = 298 K).

4. EXSY NMR spectra in Polar Solvents. Figure S2.

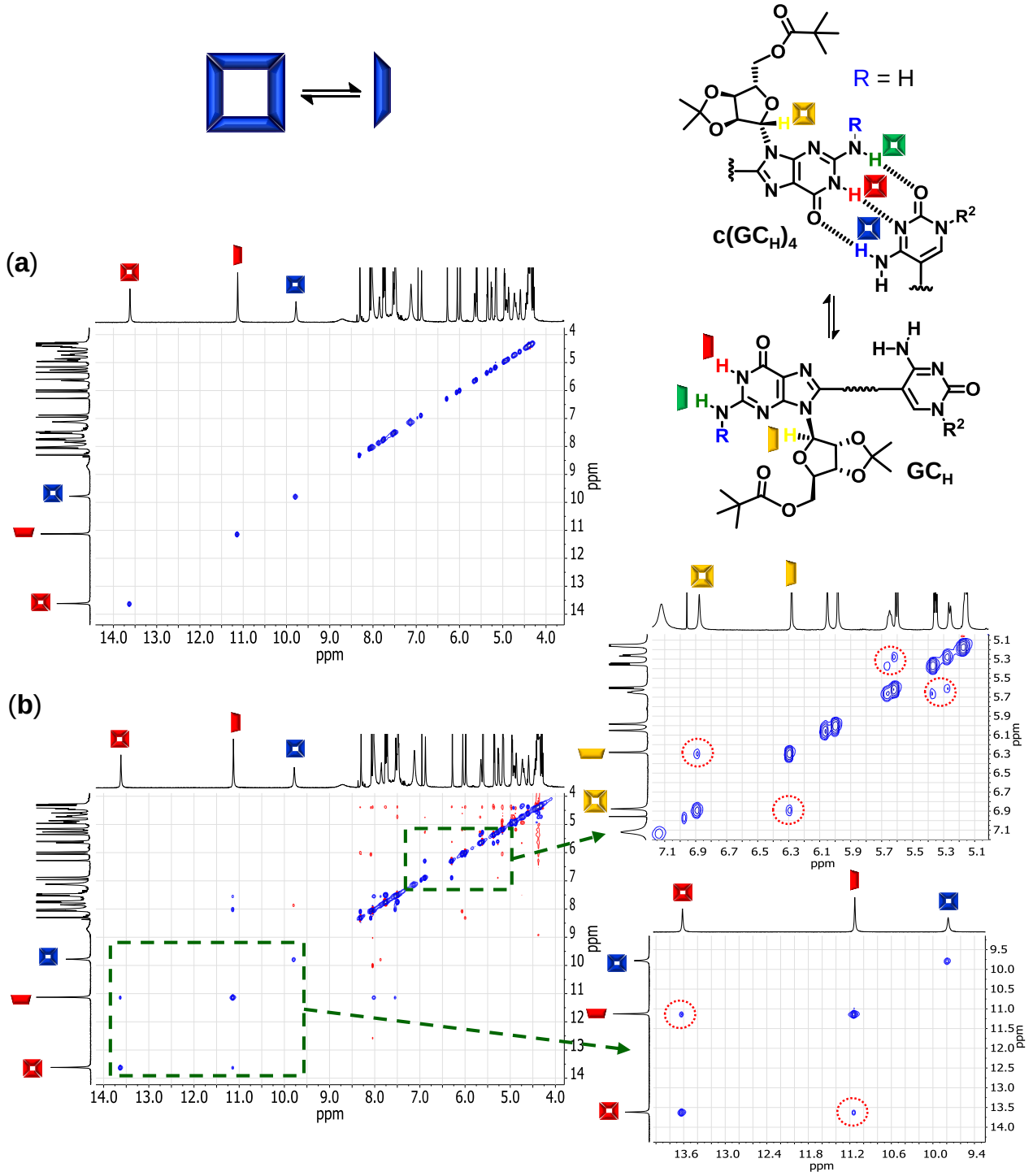

Figure S2A. 14.0-4.0 ppm region of the (**a**) NOESY spectrum of **GC$_H$** in DMF-D_7 at τ_m = 0 ms and (**b**) T-ROESY spectrum of **GC** in DMF-D_7 at τ = 100 ms. Two regions were magnified at the right: (top) ribose proton region (7.2-5.0 ppm) and (bottom) H-bonded proton region (14.0-9.5 ppm). In all cases, C = 2.0 x 10^{-2} M, T = 298 K.

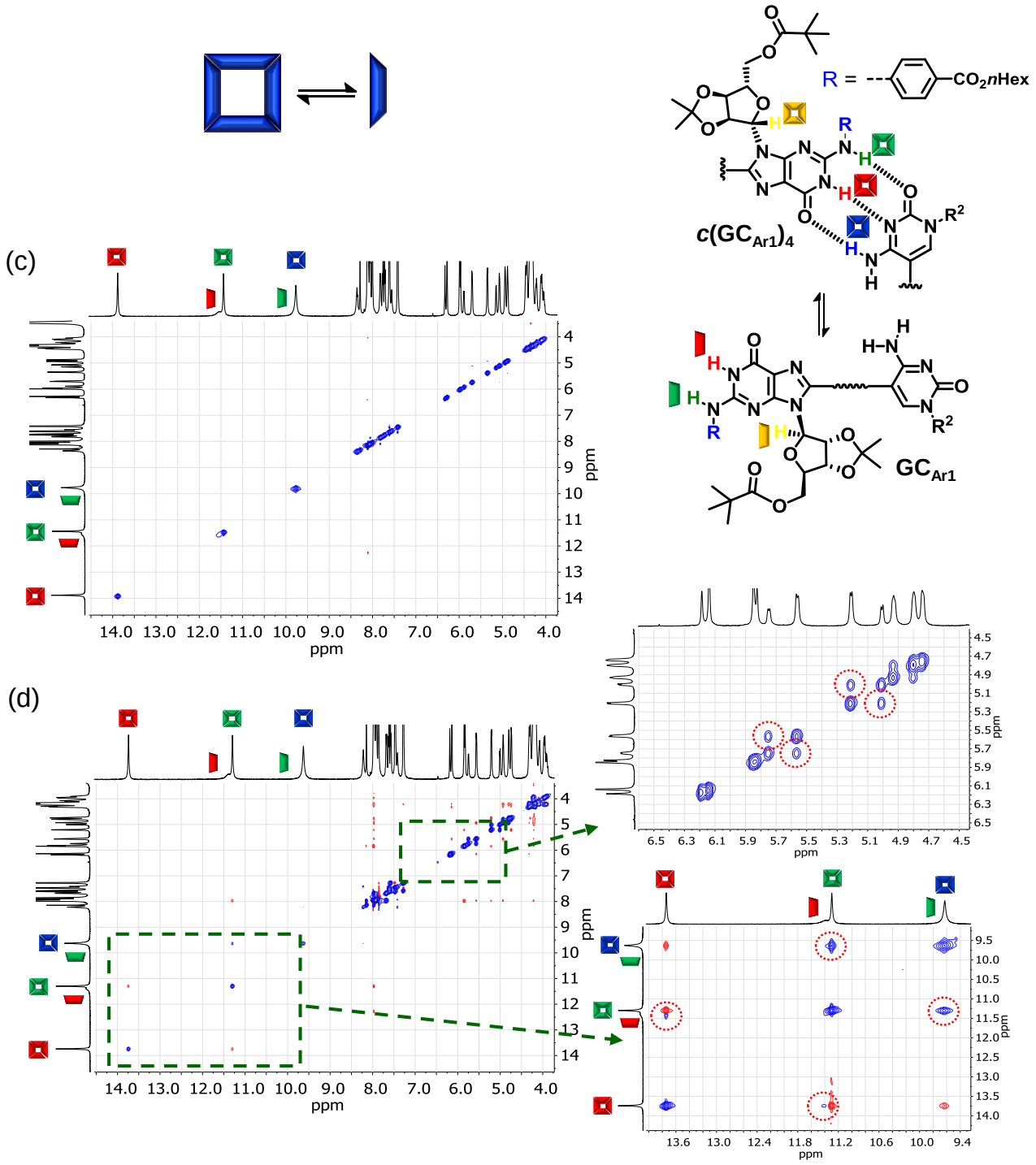

Figure S2B. 14.0-4.0 ppm region of the (**c**) NOESY spectrum of **GC$_{Ar1}$** in DMF-D_7 at τ_m = 0 ms and (**d**) T-ROESY spectrum of **GC$_{Ar1}$** in DMF-D_7 at τ = 150 ms. Two regions were magnified at the right: (top) ribose proton region (6.5-4.5 ppm) and (bottom) H-bonded proton region (14.0-9.5 ppm). In all cases, C = 2.0 x 10^{-2} M, T = 298 K.

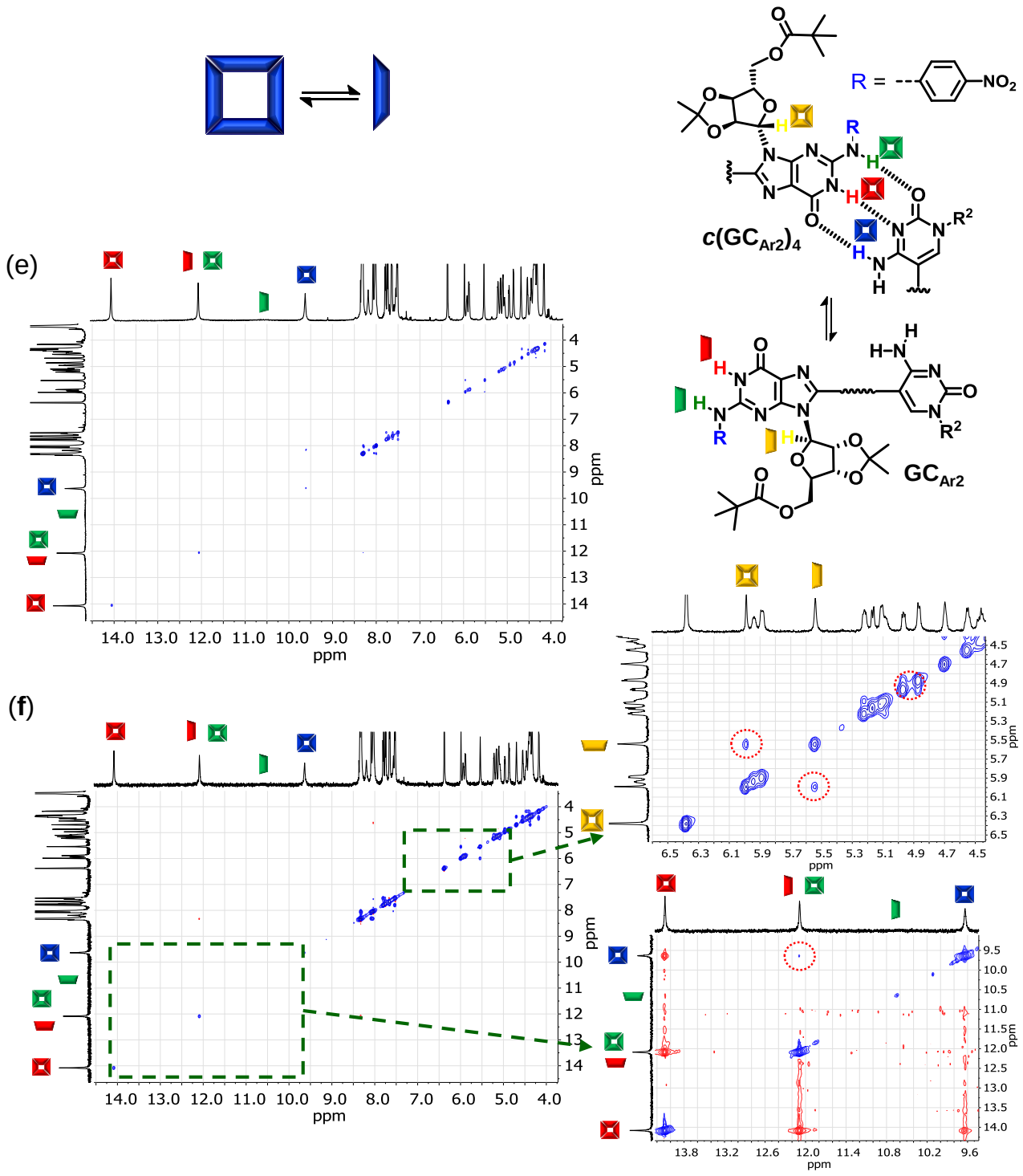

Figure S2C. 14.0-4.0 ppm region of the (**e**) NOESY spectrum of **GC$_{Ar2}$** in DMF-D_7 at τ_m = 0 ms and (**f**) T-ROESY spectrum of **GC$_{Ar2}$** in DMF-D_7 at τ = 150 ms. Two regions were magnified at the right: (top) ribose proton region (6.5-4.5 ppm) and (bottom) H-bonded proton region (14.0-9.5 ppm). In all cases, C = 2.0 x 10^{-2} M, T = 298 K.

NOESY and T-ROESY spectra show several cross peaks that correspond to the exchange of **GC** between monomer and cyclic tetramer states. Some of the ribose proton signals were considered appropriate to

calculate the exchange rate constants, since they are well-separated and correspond to C-H protons. In order to calculate the exchange rate constants, 2D NOESY spectra were taken at different mixing times and the data was analyzed in two ways:

a) Using the equations shown below, where k is the exchange rate constant, τ_m is the mixing time, X_A and X_B are the molar fractions of molecules in states A and B, respectively, I_{AA} and I_{BB} are the diagonal peak intensities, and I_{AB} and I_{BA} are the cross-peak intensities, we obtained values for k, which are the sum of the forward (association; k_1) and backward (dissociation; k_{-1}) pseudo-first order rate constants for the assembly process.

$$k = \frac{1}{\tau_m} \ln \frac{r+1}{r-1} \qquad r = 4X_A X_B \frac{I_{AA} + I_{BB}}{I_{AB} + I_{BA}} - (X_A - X_B)^2$$

b) Using the software EXSY Calc (from MestreLab Research, available at http://mestrelab.com/software/), which affords a quantitative analysis of the experimental intensities of the NMR peaks obtained in EXSY experiments to calculate the magnetization exchange rates of the exchange equilibrium. EXSY Calc directly calculates the forward (association; k_1) and backward (dissociation; k_{-1}) pseudo-first order rate constants by resolving the corresponding exchange rate matrix. Then, $k = k_1 + k_{-1}$.

The mean value obtained from both methods at different mixing times is summarized in Table 1 and S3.

5. Concentration-dependent ^{1}H NMR experiments in polar solvents. Figure S3.

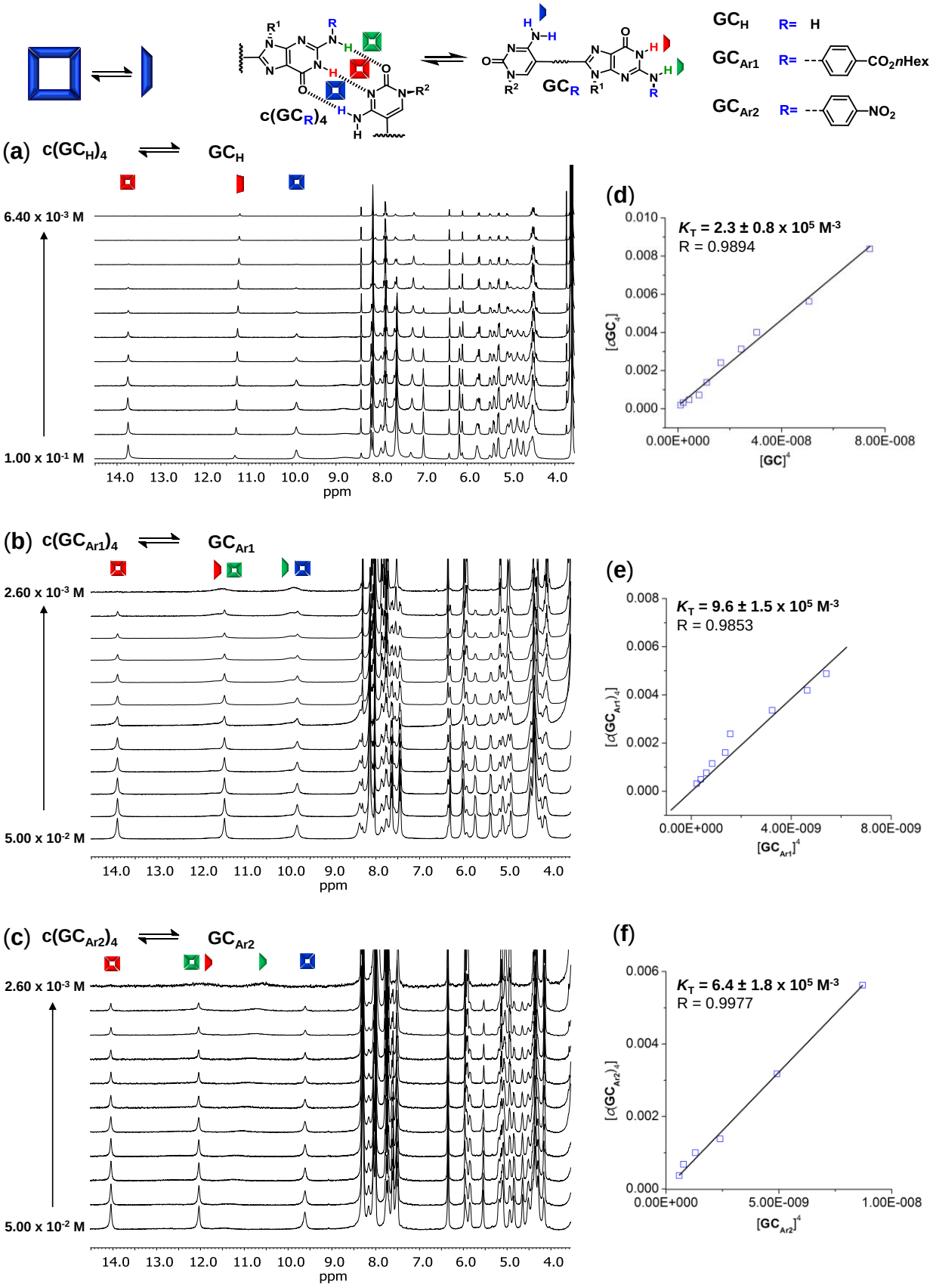

Figure S3A. 14.5-3.5 ppm region of the ^{1}H NMR spectra of (**a**) **GC$_H$,** (**b**) **GC$_{Ar1}$** and (**c**) **GC$_{Ar2}$** in pure DMF-D$_7$ as a function of the concentration (T = 298 K). (**d,e,f**) Plots of [*c***GC**$_4$] *vs* [**GC**]^4 for each product.

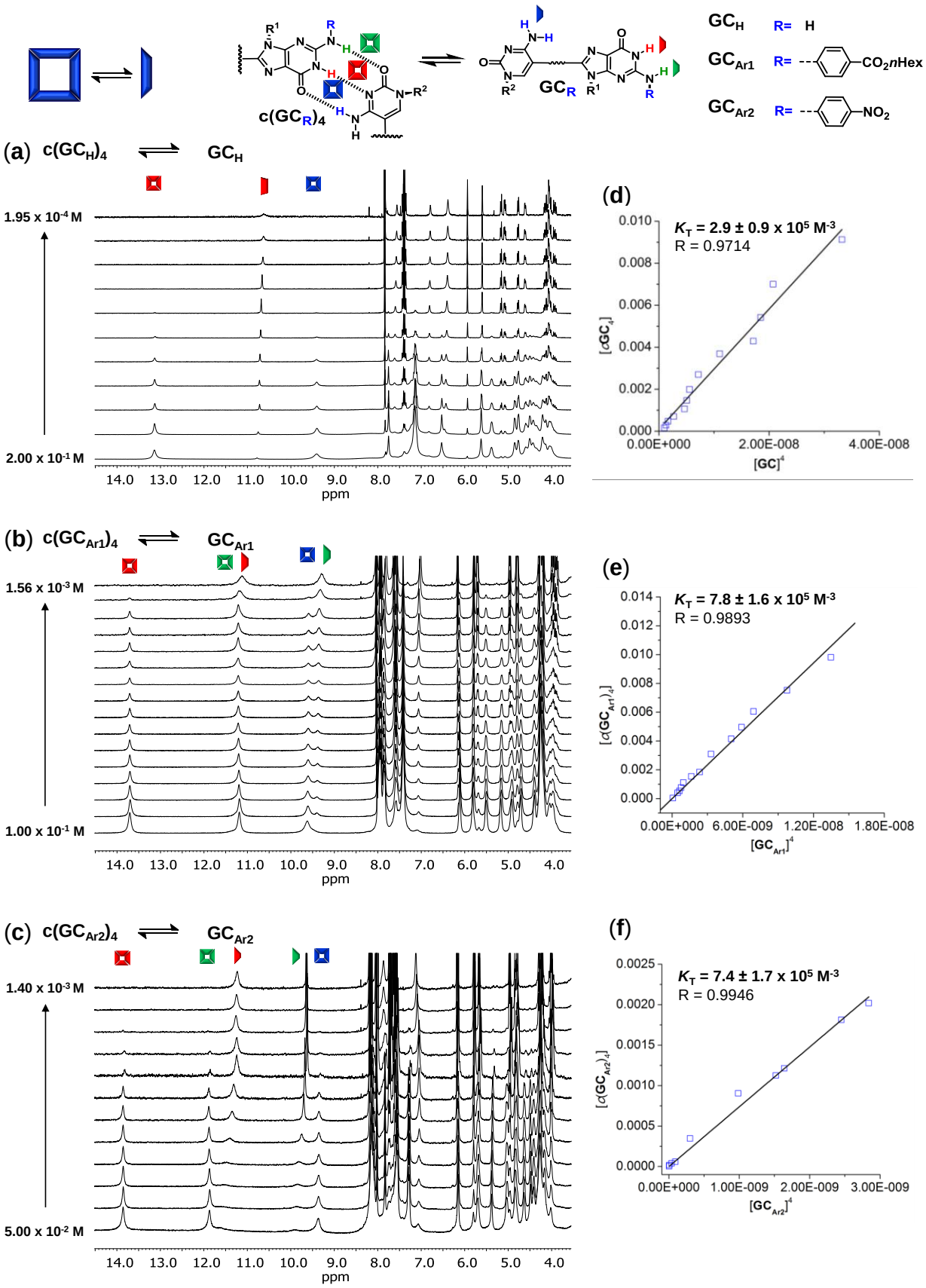

Figure S3B. 14.5-3.5 ppm region of the ^{1}H NMR spectra of (**a**) **GC$_H$,** (**b**) **GC$_{Ar1}$** and (**c**) **GC$_{Ar2}$** in a 1:1 v/v $CDCl_3$-DMSO-D_6 solvent mixture as a function of the concentration (T = 298 K). (**d,e,f**) Plots of [*c***GC**$_4$] *vs* [**GC**]^4 for each product.

Dilution experiments of **GC$_H$**, **GC$_{Ar1}$** and **GC$_{Ar2}$** in highly polar solvents revealed the presence of an equilibrium between monomer **GC** and cyclic tetramer *c***GC**$_4$. It is interesting to note that the shape and position of the G-amide and C-amine protons do not change with concentration, suggesting a very slow exchange in the NMR timescale and an “all-or-nothing“ behavior. The concentrations of **GC** and *c***GC**$_4$ were calculated in each spectrum by signal integration (at least 2 C-H proton signals for each species were averaged). Within the whole concentration range, [*c***GC**$_4$] and [**GC**]^4 follow a linear relationship (but not [*c***GC**$_4$] and [**GC**]^3 or [*c***GC**$_4$] and [**GC**]^5, supporting the formation of a tetramer) from which K_T was calculated:

$$K_T = \frac{[c\mathbf{GC_4}]}{[\mathbf{GC}]^4}$$

6. Temperature-dependent ^{1}H NMR experiments in polar solvents. Figure S4.

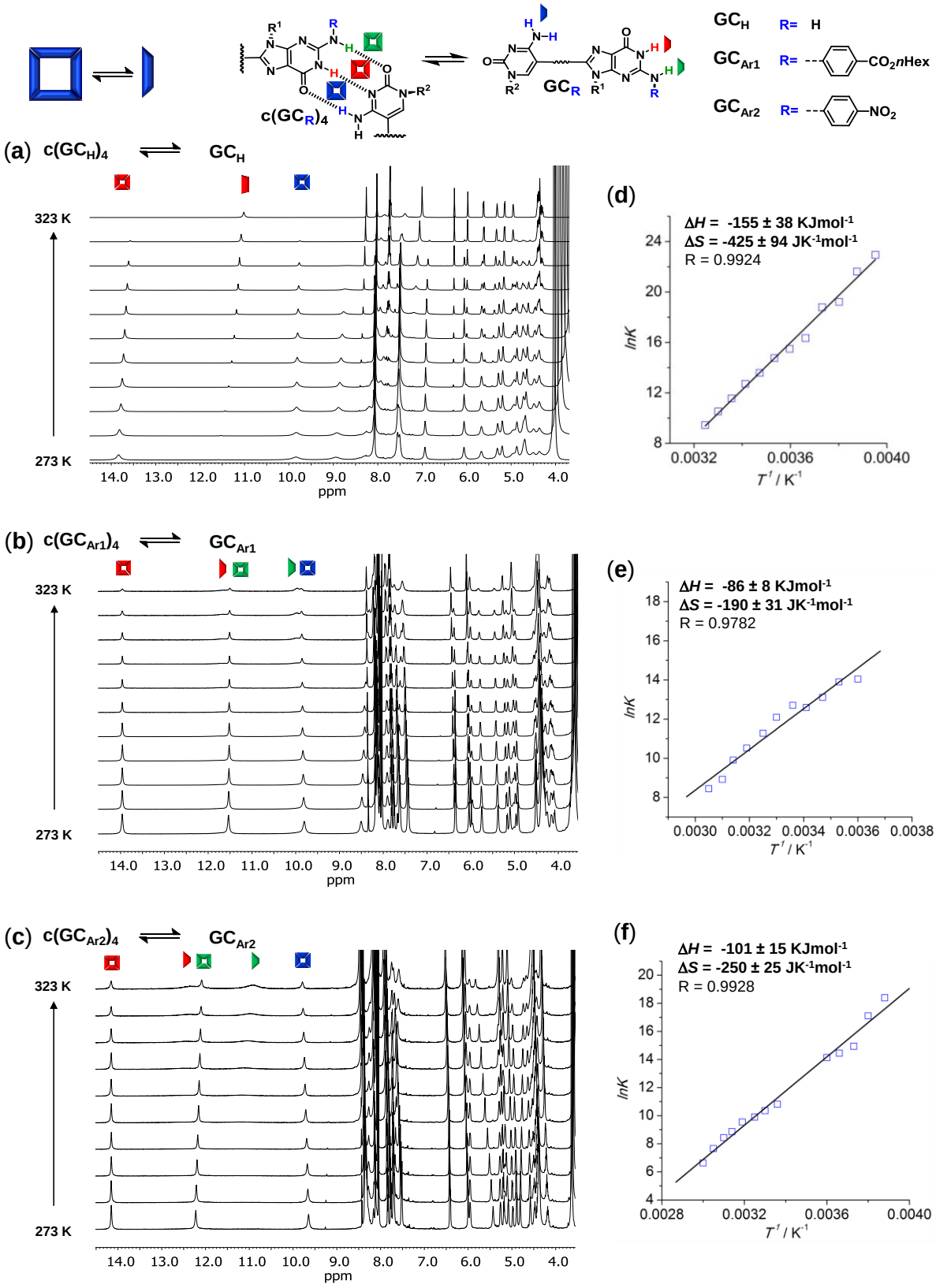

Figure S4A. 14.5-3.5 ppm region of the ^{1}H NMR spectra of (**a**) $\mathbf{GC_H}$, (**b**) $\mathbf{GC_{Ar1}}$ and (**c**) $\mathbf{GC_{Ar2}}$ in pure DMF-D_7 as a function of the temperature (*C* = 1.0 x 10^{-2} M). (**d,e,f**) Van´t Hoff analysis of the temperature dependent data for each product.

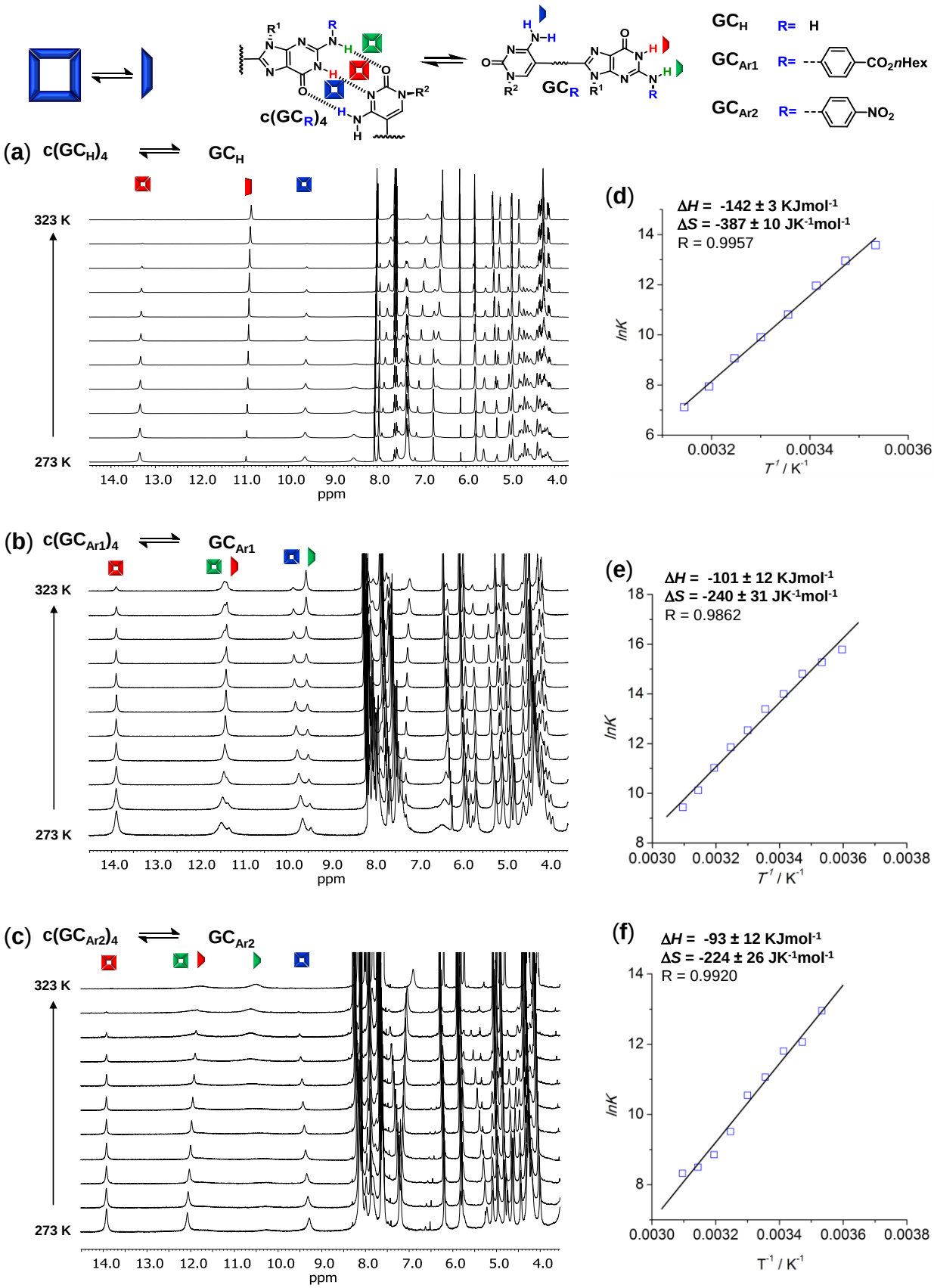

Figure S4B. 14.5-3.5 ppm region of the ^{1}H NMR spectra of (**a**) $\mathbf{GC_H}$, (**b**) $\mathbf{GC_{Ar1}}$ and (**c**) $\mathbf{GC_{Ar2}}$ in 1:1 v/v $CDCl_3$-DMSO-D_6 solvent mixture as a function of the temperature (C = 1.0 x 10^{-2} M). (**d,e,f**) Van´t Hoff analysis of the temperature dependent data for each product.

Increasing the temperature of the **GC$_H$**, **GC$_{Ar1}$** and **GC$_{Ar2}$** solutions in highly polar solvents resulted in tetramer dissociation to yield monomeric species. Please note that the shape and position of the G-amide and C-amine protons do not change significantly with temperature, indicating again a very slow exchange in the NMR timescale (even at high temperatures) and the presence of mainly the **GC** and *c***GC**$_4$ species. The concentrations of **GC** and *c***GC**$_4$ were calculated in each spectrum by signal integration (at least 2 C-H proton signals for each species were averaged) and ln*K* was plotted *vs* T^{-1} (Van´t Hoff plot), yielding ΔH and ΔS values in each solvent system:

$$\ln(K) = -\frac{\Delta H^0}{R}\left[\frac{1}{T}\right] + \frac{\Delta S^0}{R}$$

7. Concentration-dependent UV-vis and CD experiments in THF. Figure S5.

Absorption and circular dichroism (CD) spectroscopy was employed to further analyze the monomer-cyclic tetramer equilibrium. DMF or DMAC solvents are too polar and, as previously observed in ^{1}H NMR dilution experiments (see Figure S3), the monomer is the only species present below a concentration of 10^{-3} M. At the other extreme, in apolar solvents that do not compete strongly for H-bonding, like CCl_4 or toluene, the tetramer is too stable to be dissociated by concentration or temperature changes. In solvents of intermediate polarity, like THF or dioxane, we could study the cyclotetramerization equilibria in the 2 x 10^{-4}–1 x 10^{-6} M concentration regime.

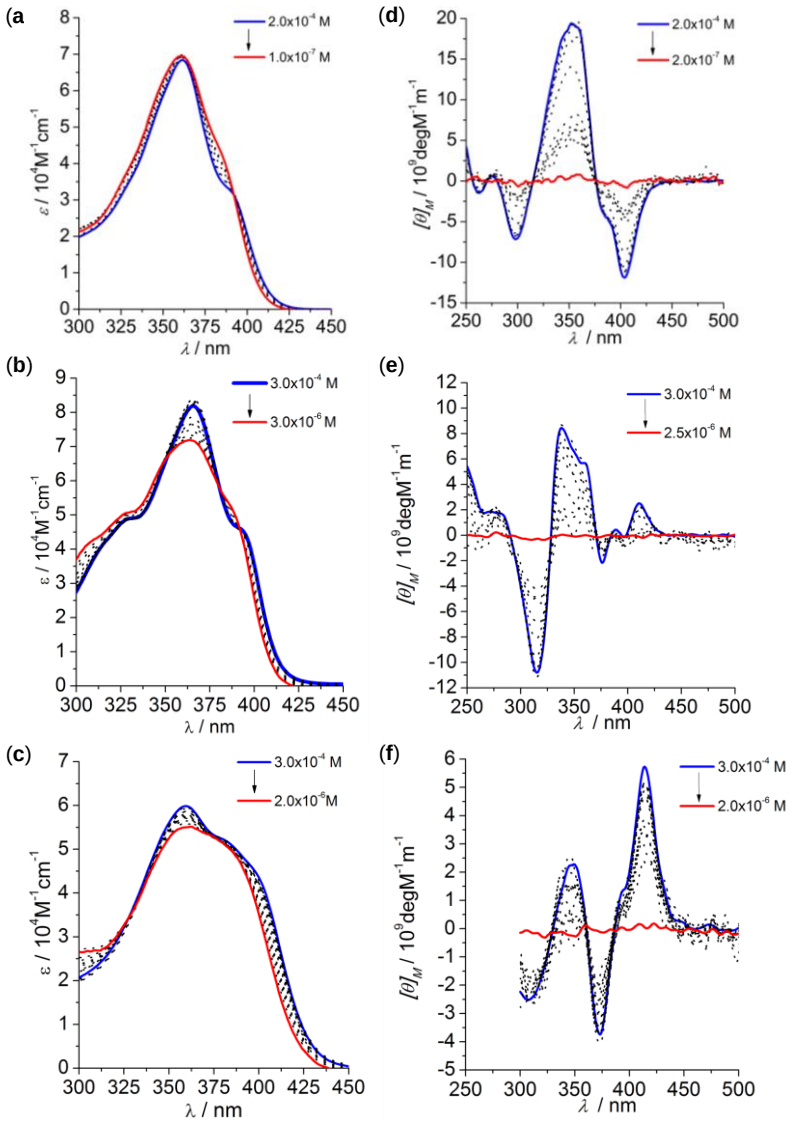

Figure S5A. Concentration-dependent UV-vis (**a**,**b**,**c**) and CD (**d**,**e**,**f**) spectra of **GC$_H$, GC$_{Ar1}$** and **GC$_{Ar2}$** in THF at 298 K.

Calculation of K_T from the spectroscopic changes experienced by **GC$_{Ar1}$** and **GC$_{Ar2}$** in THF upon association into cyclic tetramers was performed by using the software *ReactLab™ EQUILIBRIA* which is developed and commercialized by Jplus Consulting Pty Ltd (http://jplusconsulting.com/). It allows for the global fitting of multi-wavelength spectroscopic data to chemical reaction schemes, and determines all equilibrium constants in the

underlying mechanism. The analysis also yields the concentration distributions of all species and the individual spectra of all the participating species. The program, including all algorithms and the GUI frontend has been developed in Matlab and compiled to produce the final deployable application.

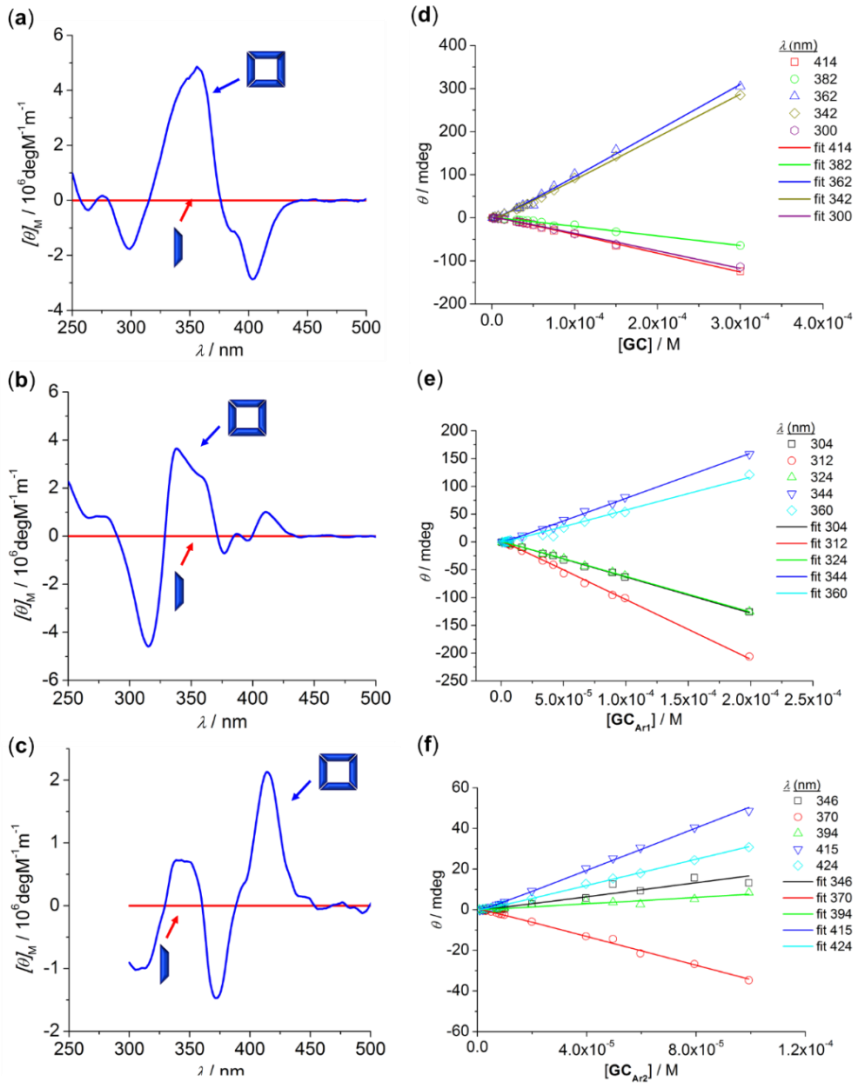

Figure S5B. (**a,b,c**) Calculated **GC_H, GC_{Ar1}** and **GC_{Ar2}** monomer (red) and tetramer (blue) as CD spectra. (**d,e,f**) Fitting of the concentration-dependent as CD data at 5 selected wavelengths.

Table S1. Concentration-dependent data fitted by *ReactLab™ EQUILIBRIA*

	Data	K_T M^{-3}
GC_H[a]	**CD**	(1.0±0.2) x10^{15}
GC_{Ar1}	**CD**	(4.6±1.2) x10^{16}
GC_{Ar2}	**CD**	(5.9±2.7) x10^{16}

[a] Reference 1b

8. Temperature-dependent UV-vis and CD experiments in THF. Figure S6.

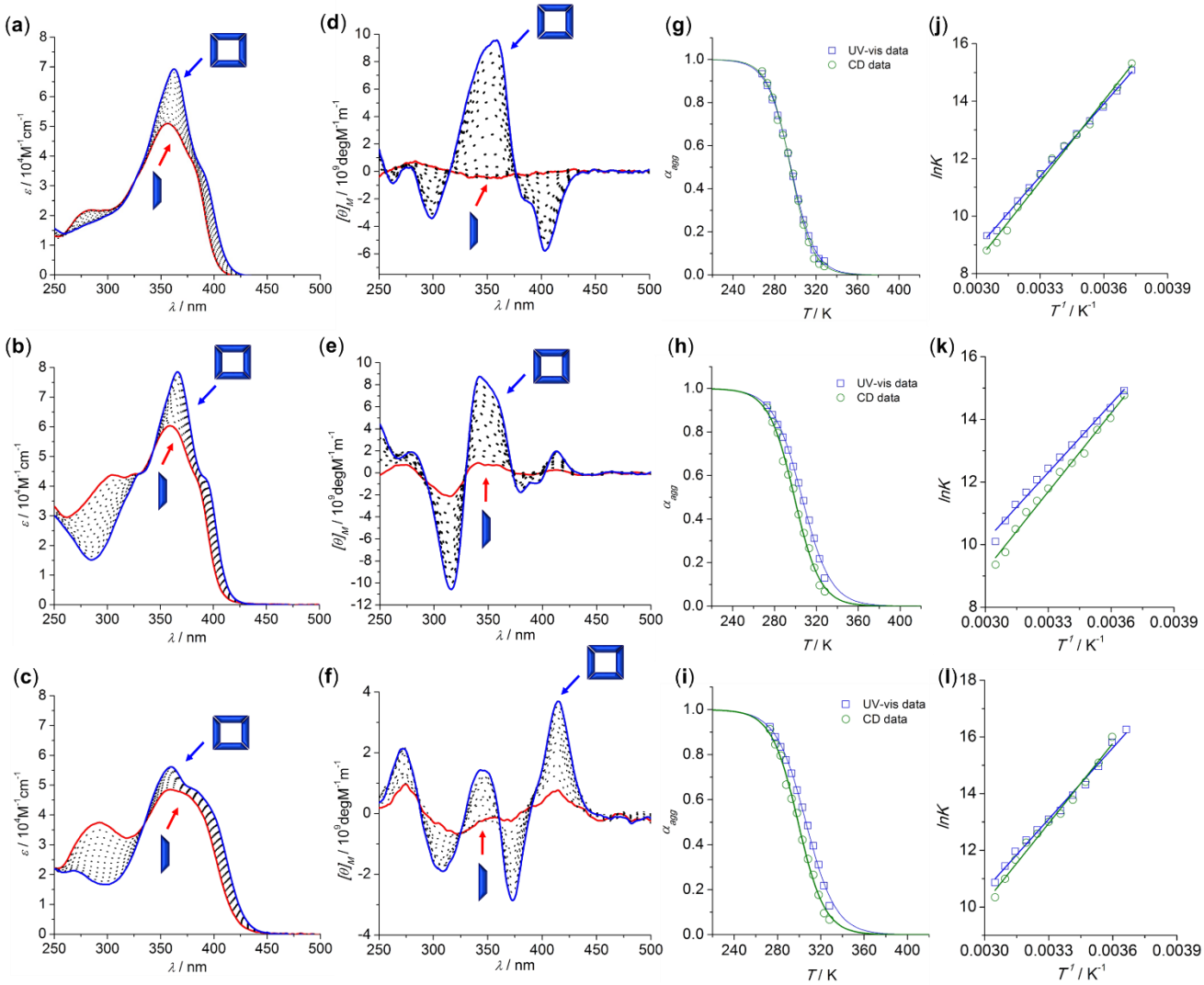

Figure S6. Temperature-dependent UV-vis (**a**,**d**,**c**) and (**d**,**e**,**f**) CD spectra. (**g**-**i**) Fitting of the cooling curves to the isodesmic model and Van't Hoff ln*K* *vs* T^{-1} plots (**j**-**l**) of $\mathbf{GC_H}$ (**a**,**d**,**g**,**j**), $\mathbf{GC_{Ar1}}$ (**b**,**e**,**h**,**k**) and $\mathbf{GC_{Ar2}}$ (**c**,**f**,**i**,**l**) in THF at 1.25 x 10^{-5} M in all cases.

It should be noted that in the set of spectra shown in Figure S6, the changes observed as a function of temperature reflect both the conformational changes of the π-conjugated system and the monomer-tetramer association equilibrium. Such conformational changes are common in oligo(phenyleneethynylene) and oligo(phenylenevinylene) molecules and are just due to planarization of the π-conjugated system at lower temperatures.[2] In concentration-dependent measurements the first effect is eliminated, and only the association equilibrium is instead observed (compare Figures 3a-b with Figures 3c-d in the text or Figures S4 and S5).

[2] (a) Jonkheijm, P.; v. d. Schoot, P.; Schenning, A. P. H. J.; Meijer, E.W. *Science* **2006**, *313*, 80-83. (b) González-Rodríguez, D.; Janssen, P. G. A.; Martín-Rapún, R.; De Cat, I.; De Feyter, S.; Schenning, A. P. H. J.; Meijer, E. W. *J. Am. Chem. Soc.* **2010**, *132*, 4710-4719.

The temperature-dependent association data was analyzed using the equal-*K* oligomerization (or isodesmic) model. [3] The use of such model needs to be considered with caution. It is a model that supposes a distribution of oligomeric species with an average degree of polymerization (DP_N) whose value depends on the temperature, the concentration and the association constant (K_{iso}). The model considers that the reversible formation of noncovalent bonds is identical for all binding events, implying that the reactivity of the end groups does not change during the supramolecular aggregation process. Thus, the equilibrium constants (K_{iso}) and Gibbs free energy changes are equal for each step of the growing aggregate. Such model is not strictly valid to fit our **GC** monomer–*c***GC**$_4$ cyclic tetramer equilibria data, since our system is not composed of a distribution of oligomers, but mainly of **GC** monomer and *c***GC**$_4$, and self-assembly is limited at the tetramer level so the system does not grow further to a high extent. However, it has proven useful and sufficiently accurate as long as some precautions are taken.[1] In order to minimize the effect of higher-order oligomers, we limited the experiments to low DP_N values, well below 4 across the whole concentration or temperature range. The association constant calculated by this model (K_{iso}) should be then interpreted as an average apparent association constant for each monomer addition step to build a given oligomer, in this case a tetramer:

$$\mathbf{GC} \overset{K_{iso}}{\rightleftharpoons} \mathbf{GC_2} \overset{K_{iso}}{\rightleftharpoons} \mathbf{GC_3} \overset{K_{iso}}{\rightleftharpoons} \mathbf{GC_4} \qquad K_T = K_{iso}^3$$

Therefore, a tetramerization constant using the isodesmic model equals $(K_{iso})^3$. On the other hand, the free energy, enthalpy and entropy changes for a tetramerization process would be three times those obtained from the equal-*K* model.

Assuming a two-state equilibrium, the degree of polymerization or the molar fraction of aggregated species $\alpha_{agg}(T)$ is related to temperature by means of a sigmoidal relation. The number-averaged degree of polymerization $DP_N(T)$ can be calculated from $\alpha_{agg}(T)$:

$$DP_N = \frac{1}{\sqrt{1-\alpha_{agg}(T)}}$$

Taking into equation:

$$\alpha_{agg} = 1 - \frac{2Kc_T + 1 - \sqrt{4K(T)c_T + 1}}{2K^2c_T^2}$$

This expression can be related to the equilibrium constant *K* and the total concentration of molecules c_T via:

$$DP_N = \frac{1}{\sqrt{1-\alpha_{agg}(T)}} = \frac{1}{2} + \frac{1}{2}\sqrt{4K(T)c_T + 1}$$

This is equal to equation:

[3] (a) Smulders, M. M.; Nieuwenhuizen, M. M. L.; De Greef, T. F. A.; Van der Schoot, P.; Schenning, A. P. H. J.; Meijer, E. W. *Chem. Eur. J.* **2010**, *16*, 362-367. (b) De Greef, T. F. A.; Smulders, M. M. J.; Wolffs, M.; Schenning, A. P. H. J.; Sijbesma, R. P.; Meijer, E. W. *Chem. Rev*. **2009**, *109*, 5687-5754.

$$DP_N = \frac{c_T}{c_N} = \frac{c_T(1 - Kc_1)}{c_1} = \frac{1 + \sqrt{4Kc_T + 1}}{2}$$

Aside from, as explained above, limiting our experiments to low DP_N values, the analysis of the temperature-dependent data required an additional correction. As explained above, the changes observed as a function of temperature in THF or dioxane reflect both the conformational changes due to planarization of the π-conjugated system at low temperatures and the monomer-tetramer association equilibrium. In order to subtract the first effect, we normalized each set of data at the corresponding wavelength using the changes experienced by the system in the fully dissociated (DMAC) or fully associated (CCl_4) state, where only the intrinsic conformational changes are observed with temperature. This kind of correction has been employed before by us[1b] and others in oligo(phenylenevinylene) aggregation processes.[2]

Table S2 displays all the thermodynamic data obtained by fitting our temperature-dependent experiments.

Table S2. Temperature-dependent data fitted by the isodesmic model

	Data	***λ*** nm	K_{iso} [a] M^{-1}	R^2	K_T [a,b] M^{-3}	T_M K	DP_N [a]	$\Delta H°$ [a,c] $kJmol^{-1}$	$\Delta S°$ [a,c] $Jmol^{-1}K^{-1}$	$\Delta G°$ [a,d] $KJmol^{-1}$	***R***
GC_H [e]	**UV-vis**	362	$1.5x10^5$	0.999	$3.4x10^{15}$	296	1.3	-70.1±1.0	-136.7±3.2	-29.4±2.0	0.998
	CD	347	$1.6x10^5$	0.996	$4.0x10^{15}$	295	1.4	-78.1±2.0	-164.5±6.8	-29.1±4.0	0.992
GC_{Ar1}	**UV-vis**	359	$3.6x10^5$	0.996	$4.7x10^{16}$	306	1.7	-60.9±1.9	-98.6±6.4	-31.5±3.8	0.990
	CD	360	$2.2x10^5$	0.994	$1.1x10^{16}$	299	1.5	-69.6±2.1	-132.6±7.2	-30.1±4.3	0.990
GC_{Ar2}	**UV-vis**	375	$6.6x10^5$	0.994	$2.9x10^{17}$	314	2.0	-69.7±3.0	-121.2±6.4	-33.6±3.8	0.992
	CD	415	$6.0x10^5$	0.990	$2.2x10^{17}$	312	1.9	-78.2±3.0	-150.4±9.8	-33.4±6.0	0.985

[a] Data at 298 K. [b] Calculated as $K_T = (K_{iso})^3$. [c] Using Van´t Hoff equation: $lnK = -\frac{\Delta H°}{RT} + \frac{\Delta S°}{R}$; R = 8.3144621 $JK^{-1}mol^{-1}$. [d] Using Gibb's equation: $\Delta G° = \Delta H° - T\Delta S°$. [e] Reference 1b.

The tetramerization constants (K_T) calculated from concentration or temperature measurements, using absorption or CD spectroscopy, and employing any fitting method (*ReactLab™ EQUILIBRIA* or the Isodesmic model, repectively) as explained above, are all in acceptable accordance and around $K_T = 10^{15}$-10^{17} M^{-3}. With regards to the thermodynamic parameters obtained from the temperature-dependent experiments, it is important to note that K_{iso}, K_T, ΔH, ΔS and ΔG values calculated at 298 K (where $DP_N \approx 1.3$) are in good accordance independently of the spectroscopic technique employed or the wavelength chosen. At least 5 wavelengths were tested for each technique, all of them leading to similar results. Averaged K_T, and the ΔH and ΔS values for the isodesmic process were calculated from all these data and exported for a tetramerization process to Table 1 in the text and Table S3.

9. Overview of thermodynamic and kinetic parameters calculated for the cyclotetramerization process of GC_H, GC_{Ar1} and GC_{Ar2} in different solvents. Table S3.

Solvent	Compd.	K_T[a] M^{-3}	ΔH[b] $kJmol^{-1}$	ΔS[b] $Jmol^{-1}K^{-1}$	τ[c] s^{-1}	C_{50}[d] M	T_{50}[e] K
1:1 $CDCl_3$-DMSO-D_6	GC_H	$2.9 \pm 0.9 \times 10^5$	-142 ± 3	-387 ± 10			
	GC_{Ar1}	$7.8 \pm 1.6 \times 10^5$	-101 ± 12	-240 ± 31			
	GC_{Ar2}	$7.4 \pm 1.7 \times 10^5$	-93 ± 12	-224 ± 26			
DMF-D_7	GC_H	$2.3 \pm 0.8 \times 10^5$	-155 ± 38	-425 ± 94	3.0 ± 0.7		
	GC_{Ar1}	$9.6 \pm 1.5 \times 10^5$	-86 ± 8	-190 ± 31	7.1 ± 0.9		
	GC_{Ar2}	$6.4 \pm 1.8 \times 10^5$	-101 ± 15	-250 ± 25	3.8 ± 0.3		
THF	GC_H	$1.0 \pm 0.2 \times 10^{15}$	-225 ± 44	-465 ± 126		6.00×10^{-6}	295
	GC_{Ar1}	$4.6 \pm 1.2 \times 10^{16}$	-196 ± 30	-347 ± 145		3.86×10^{-6}	303
	GC_{Ar2}	$5.9 \pm 2.7 \times 10^{16}$	-221 ± 55	-407 ± 150		3.01×10^{-6}	313

[a] From dilution experiments (Figures S3 and S5). [b] From a Van't Hoff analysis of the cooling experiments (Figures S4 and S6). [c] From EXSY experiments. (Figure S2). [d] Concentration or [e] Temperature at which half of the molecules are assembled into cyclic tetramers.